OAA Technical Memorandum ERL ARL-83

COMPARISON OF ESTIMATED AND OBSERVED VALUES FOR SOLAR RADIATION AT THE SURFACE OF THE AFRICAN CONTINENT

J. K. Nimira

Air Resources Laboratories
Silver Spring, Maryland
January 1980

noaa NATIONAL OCEANIC AND ATMOSPHERIC ADMINISTRATION / Environmental Research Laboratories

NOAA Technical Memorandum ERL ARL-83

COMPARISON OF ESTIMATED AND OBSERVED VALUES FOR SOLAR RADIATION AT THE SURFACE OF THE AFRICAN CONTINENT

J. K. Nimira
Geophysical Monitoring for Climatic Change

Air Resources Laboratories
Silver Spring, Maryland
January 1980

UNITED STATES DEPARTMENT OF COMMERCE
Philip M. Klutznick, Secretary

NATIONAL OCEANIC AND ATMOSPHERIC ADMINISTRATION
Richard A. Frank, Administrator

Environmental Research Laboratories
Wilmot N. Hess, Director

CONTENTS

TERMS USED IN THE STUDY

A_v	Annual variability
CA	Cloud cover (tenths of sky cover)
C_f	Correction factor for seasonal and latitudinal differences
C_{ff}	Collective correction factor
C_r	Ratio of low clouds to total cloud cover
D_c	Total diffuse solar radiation, cloudy sky (W m^{-2})
D_M	Diffuse component due to multiple reflection (W m^{-2})
D_o	Total diffuse solar radiation, clear sky (W m^{-2})
d_e	Deviation of estimated from observed solar radiation (W m^{-2})
E_c	Effective cloudiness (tenths of sky cover)
G_c	Global solar radiation, cloudy sky (W m^{-2})
G_o	Global solar radiation, clear sky (W m^{-2})
g	Acceleration of gravity (m s^{-2})
H	Theoretical daylight length (hours)
H*	Day length (min)
h_i	Height of level i (km)
I	Direct solar radiation, clear sky (W m^{-2})
I_c	Direct solar radiation, cloudy day (W m^{-2})
I_o	Solar radiation at the top of the atmosphere normal to the solar beam and at actual Earth-Sun distance (W m^{-2})
I_o (Θ)	Solar radiation at the top of the atmosphere at latitude Θ, annual mean (W m^{-2})
I_o (Θ, M)	Mean solar radiation at the top of the atmosphere at latitude Θ and for the month M (W m^{-2})

L_f	Latitudinal correction factor
M	Air mass at standard temperature and pressure
m*	Air mass reduced to relevant level
N	Theoretical possible duration of sunshine (hours)
n	Measured duration of sunshine (hours)
q	Specific humidity (g kg^{-1})
r	Earth's radius vector
r_{ms}	Root mean square error
S_R	Solar radiation component resulting from molecular (Rayleigh) scattering (W m^{-2})
S_a	Solar radiation component due to aerosol scattering (W m^{-2})
S_{da}	Solar radiation component due to dry aerosol scattering (W m^{-2})
S_f	Seasonal correction factor
S_o	Solar constant (1353.6 W m^{-2})
S_{wa}	Solar radiation component due to wet aerosol scattering (W m^{-2})
s	Standard deviation
T_i	Transmission function resulting from either absorption or scattering by i; stands for ozone (O_3), oxygen (O_2), carbon dioxide (CO_2), water absorption and scattering (W_a, W_s), aerosol absorption and scattering (A_a, A_s), dry and wet aerosol scattering (A_d, A_w), and Rayleigh scattering (R_s).
$T_{w,i}$	Water vapor transmittance at grid point i
$T_{w,SI}$	Water vapor transmittance at Swan Island
t	Temperature (t_o = standard °C)
U_i	Optical thickness (cm) with index i standing for the component in question

v	Coefficient of variability
W_c	Effective precipitable water
W_∞	Precipitable water
z	Zenith angle (degrees)
α_a	Atmospheric albedo
α_s	Surface albedo
β	Ratio of forward scattering to total scattered radiation
Δ	Deviation of (n + CA) from unit
δ	Sun's declination (degrees)
ρ	Atmospheric pressure (ρ_o = standard, mb)
Θ	Latitude (degrees)
η	Angström's coefficient
ω_o	Single scattering albedo (allocates the fraction of radiation attenuated by aerosols)

COMPARISON OF ESTIMATED AND OBSERVED VALUES FOR SOLAR RADIATION AT THE SURFACE OF THE AFRICAN CONTINENT

J. K. Nimira

ABSTRACT. Solar radiation fluxes at the surface of the African continent were estimated by three methods. The methods used cloud data derived from satellite measurements, observed sunshine hour data, and data on several other parameters measured at 57 ground stations throughout Africa. The estimated values were then compared with actual observed global solar radiation values from 10 selected stations. The percentage deviation between estimated and observed values was generally less than ±15%.

1. INTRODUCTION

Fossil fuel, the main commercial source of energy, must be supplemented if we are to keep pace with the ever-increasing demand for energy. Solar energy is one possible supplement. Unfortunately, unlike many other meteorological parameters, solar energy quantities have not been routinely or widely observed in the past, and where observations are available they generally do not cover a sufficient length of time. This makes interpretation inadequate and interpolation unreliable.

However, solar energy fluxes can be estimated by using the available data on other meteorological parameters. The purpose of the present study, focusing on Africa, is to determine how reliable these estimates might be, by comparing them with actual observations of solar fluxes. The data used for these estimates came from satellite observations or from ground-based meteorological observations. This study examines three approaches to working with these data, the regression method (R method), the semi-empirical transfer method with cloud data (ST-C method), and the semi-empirical transfer method with cloud and sunshine data (ST-CS method).

Cloud and sunshine data have been used extensively in radiation estimates (Angstrom, 1924, Kondratyev, 1969: Baker and Haines, 1969; Suckling and Hay, 1977; Hanson, 1976). Regional or local energy budget component studies commonly use regression relationships between the observed radiation component and cloud and/or sunshine data. The regional or local regression equations thus developed are localized, and any attempt to extrapolate them to other regions may result in large errors (Baker and Haines, 1969). In the present study correction terms are applied in an attempt to reduce these errors.

The semi-empirical transfer method is aided by the increase in both coverage and volume of upper air data. The method has been applied by Katayama (1966), Sasamori et al. (1972), and Hoyt (1976), to mention just a few. In this study, data on the following parameters were used to estimate solar radiation components reaching the surface of Africa: climatological mean monthly air temperature and

dew point depression vertical atmospheric profiles, spectroscopically active atmospheric constituents, sunshine hours, mean annual surface albedo, and cloud data derived from satellite observations (Sadler, 1968).

The estimates gained from using these methods were compared with data on observed solar radiation from 10 stations in different climatic regions throughout the continent of Africa (see fig. 1). Results from both the R and ST methods show agreement in long-term monthly mean values to within ±20%. Further, it was found that the R method, which also uses the satellite-derived cloud data, gives better results if data for all the period of study are treated as one sample, that is, without regard to seasonal grouping. This may be because the data set was not large enough to form statistically stable seasonal samples. The ST technique was found to perform better than the R method and ST-CS better than ST-C. Percentage deviations of estimates from observed mean monthly global solar radiation for the ten selected stations are generally less than ±15%.

For background information, a discussion of the general climatological features of Africa has been included as an appendix to this report.

2. DATA

The "satellite-derived" cloud data were derived by Sadler (1968; also J. C. Sadler, University of Hawaii, Honolulu, Hawaii, personal communication) from operational nephanalyses based on digital satellite data and prepared by the Data Processing and Analysis Division of the National Environmental Satellite Center of ESSA. From these data, a cloudiness value was assigned to the central point of each square of the 2.5-degree latitude-longitude grid. Appropriate areal weighting was done where different neph categories of cloudiness covered a grid square. No actual satellite pictures were used in the cloud data deductions. The data were for 1965 through 1973.

The grid covers a far greater area than that used in conventional cloud observation methods; thus, considerable smoothing of data is required. The cloud data set does not distinguish between different cloud forms. Hence, for any meaningful estimates of solar radiation and for the R method in particular, a high degree of homogeneity of cloudiness both in form and amount is essential. Satisfying this need was the basis for choosing a U.S. weather station on an isolated tropical island, Swan Island (17°24'N, 83°56'W) in the West Indies, as the base station at which a regression relationship between ground-observed global solar radiation and satellite-derived data was to be developed.

Monthly mean values of the vertical profiles of air temperature and dew point depression for the period 1965 to 1972 were taken from throughout Africa (fig. 1) and used to estimate the specific humidity profiles and then precipitable water W_∞ as

$$W_\infty = \frac{1}{g} \int_{\rho}^{\rho_o} q\,dp \quad . \tag{1}$$

Figure 1.--Stations used in the study for ● precipitable water and sunshine hours, Δ comparison of observed and estimated solar radiation.

The temperature data were obtained from U.S. Department of Commerce (1965-1972). Beyond levels where temperature dew point depression values were not available, the empirical formula of Gann (Kondratyev, 1973), given as

$$q = q_{h_1} * 10^{-(h_2 - h_1)/6.3} , \qquad (2)$$

was applied. In any case, a -40°C temperature was taken as the level of zero water vapor. This is on the assumption that solar energy absorption in the water continuum is negligible.

In the case of surface albedo, it was assumed that there is very little seasonal variation over the continent of Africa; hence, a mean annual value for each central grid point would suffice. Central grid point values were estimated from the results of Rockwood and Cox (1978) for much of the northern section of Africa. For the other parts of the continent, Kondratyev's (1969) values of albedo for different surfaces and the basic climatic classification for the continent of Africa were used to extend Rockwood and Cox's work and generate each grid point value.

For ozone, mean monthly 5° latitudinal values for 1957 through 1975 (see table 1) were obtained from S. Oltmans (NOAA/ERL, Boulder, Colo., personal communication, 1978). The carbon dioxide mean monthly estimates were taken from Pearman (1978), with a mean annual value of 330 ppm.

Except for carbon dioxide, ozone, albedo, and cloud data values, all parameters were estimated only for the mid-seasonal months of January, April, July, and October. The estimated values were then used for each pair of surrounding months as well.

Before being subjected to regression analysis the measured global radiation data from Swan Island were corrected for instrument degradation, calibration, and International Pyrheliometric Scale (IPS) scale conversion. The corrected data were then normalized and reduced to the equatorial latitude through the correction factor C_f as follows:

$$C_f = S_f * L_f = \frac{I_o\,(EQ,M)}{I_o\,(L,M)} * \frac{I_o\,(EQ)}{I_o\,(L)} . \qquad (3)$$

Derivation of the Angstrom coefficient (η) in equations 27-30 required a knowledge of cloud types. However, the climatology of amounts of various cloud types for given locations is unavailable, except for the data in Sasamori et al. (1972). Although these are more relevant to ocean areas, it was thought that they would suffice.

The stations used in the determination of sunshine and precipitable water are shown in fig. 1. For January, April, July, and October, mean monthly values were calculated for the period of study, and these were used to construct isolines for each monthly data set throughout the continent of Africa. From these maps values could be assigned to each midpoint of the grid. In the case of surface albedo, the data points were originally based on the data for major climatic zones. For other data parameters (carbon dioxide and ozone) latitudinally averaged values were used.

Table 1.--Total ozone amounts (ppm)

Latitude	Month J	F	M	A	M	J	J	A	S	O	N	D
30° N	300.4	297.7	308.0	312.0	309.4	297.4	280.9	273.9	269.2	263.4	263.8	271.9
25° N	267.7	246.5	285.6	294.8	294.7	284.0	271.0	266.0	261.9	255.7	254.4	257.8
20° N	257.8	265.2	273.8	282.6	284.5	275.9	263.3	260.4	256.1	250.5	248.0	249.4
15° N	247.8	253.8	261.9	270.3	274.2	267.8	255.6	254.8	250.2	245.2	241.5	240.9
10° N	242.9	249.0	254.6	263.8	267.2	262.0	252.2	251.0	245.3	244.8	240.7	239.9
5° N	238.0	244.1	247.3	257.3	260.1	256.2	248.7	247.2	240.4	244.4	237.9	238.8
0°	239.9	243.5	246.2	253.6	255.0	253.2	245.6	249.2	245.7	249.8	245.5	243.2
5° S	241.8	242.9	245.0	249.8	249.8	250.2	242.5	251.2	251.0	255.1	251.0	247.5
10° S	246.8	246.3	247.1	250.8	250.7	252.5	250.5	256.9	257.9	262.6	257.7	247.5
15° S	251.8	249.6	249.1	251.8	251.6	254.7	258.5	262.6	264.8	270.1	264.3	247.5
20° S	258.6	255.9	253.9	255.2	257.2	262.1	266.6	271.9	274.1	280.0	274.1	260.4
25° S	265.4	262.2	258.7	258.6	262.7	269.4	274.6	281.2	283.4	289.8	283.8	273.2
30° S	281.5	268.7	265.6	263.2	265.8	279.4	283.8	292.2	294.3	300.9	295.1	292.3
35° S	297.5	275.1	272.5	267.8	268.9	289.3	293.0	303.1	305.2	312.0	306.4	291.4

3. THEORY

3.1 Regression Analysis

The corrected and normalized Swan Island global radiation and satellite cloud data were subjected to regression analysis. For application of the Swan Island regression equation to the continent of Africa (or any other place for that matter) any differences in atmospheric constituents active in modification of solar energy would affect the estimates. Assuming that water vapor is the most variable of the effective atmospheric constituent absorbers of solar energy, an attempt was made to correct for the monthly differences in precipitable water between Swan Island and locations on the continent of Africa. Further, it was assumed that dust-loading differences affect only redistribution of components, i.e., with aerosols there is more scattering and very little absorpotion. For the individual components of solar radiation, however, this assumption may need further consideration.

Given the above, a collective factor C_{ff} to be applied to the regression equation at each grid point on the continent of Africa was calculated as follows:

$$C_{ff} = \frac{T_{W,i}}{T_{W,SI}} * (1/C_f) \quad . \tag{4}$$

The necessity for $1/C_f$ arises from the fact that Swan Island measured radiation data were reduced to equatorial latitude and corrected for seasonal variations prior to regression analysis.

3.2 Semi-Transfer Method

As solar radiation traverses the atmosphere, scattering, absorption, and reflection take place, resulting in reduced intensities of the direct beam, and in most cases increasing the scattered component. The scattered radiation will be increased in preferential directions, depending on the nature of these processes. Estimates of various components of solar radiation are generally deduced semi-empirically in terms of integral transmittances and absorption ratios.

Of the atmospheric constituents, only water vapor, ozone, carbon dioxide, and oxygen, in decreasing order of effectiveness, need be considered as solar radiation absorbers. Aerosols are treated as scatterers only in the present study.

3.2.1 Transmittances

The transmittances used in the study have been empirically derived by various workers.

Water Vapor. Lacis and Hansen (1974) have given water vapor transmittance as

$$T_{W_a} = 1 - \{0.29\ W_\infty / ([1 + 14.15\ W_\infty]^{0.635} + 0.5925\ W_\infty)\} \quad . \tag{5}$$

Equation 5 is for standard conditions. For any other condition the effective precipitable water vapor W_∞ is replaced by W_c:

$$W_c = W_\infty \left(\frac{\rho}{p_o}\right)^{0.75} \left(\frac{t_o}{t}\right)^{0.5} . \qquad (6)$$

Ozone. The ozone absorption functions are given by Lacis and Hansen (1974) for the two major absorption spectral ranges, namely ultraviolet (<.35 μm) and visible (0.5-0.7 μm):

$$T_{O_3} = 1 - \{0.1082*(U_{O_3})/(1+13.86) \times (U_{O_3})^{0.805} +$$

$$0.00658*(U_{O_3}') \; 1 + [10.36*(U_{O_3}) + 0.002118* (U_{O_3})/ \qquad (7)$$

$$[1 + 0.0042* (U_{O_3}) \; 0.00000323* (U_{O_3})\} .$$

The first two terms in the curl brackets are for ultraviolet range; the remaining terms cover the visible range.

Rayleigh Scattering. Davies et al. (1975) give the Rayleigh scattering transmission function as

$$T_{R_s} = 0.972 - 0.08262M + 0.00933M^2 - 0.0095M^3 + 0.0000437M^4 . \qquad (8)$$

Aerosol Scattering and Absorption. Whether aerosols absorb a reasonable amount of solar radiation in comparison to their scattering remains unanswered in detail. Robinson (1962) gives a good account of the problem. Many authors (e.g., Davies et al., 1975) have assumed that absorption and scattering by aerosols are comparable. This assumption is highly questionable but, because of the simplicity it offers for calculations and in the absence of a better solution, it suffices. The truth of the assumption depends on the natural aerosols. Chemical aerosols, like those from industries and other anthropogenic sources, are likely to absorb an appreciable amount of solar radiation. On the other hand, Robinson (1962) shows that natural dust absorbs very little.

Shape and size are the two dominant factors in scattering by aerosols. In the atmosphere, however, whether the aerosol is hygroscopic or not will also significantly affect the scattered radiation. This also affects the size of the aerosol particles as well as altering their absorption properties. In the present study the transmission function for the aerosols is calculated according to Katayama (1966).

For scattering by dry aerosols

$$T_{A_d} = 1 - 0.9^{m*} \qquad (9)$$

where $m* = M \, \rho/\rho_o$.

For scattering by wet aerosols

$$T_{A_w} = 1 - 0.975^{MW_\infty} . \quad (10)$$

Finally, for total aerosol scattering

$$T_{A_s} = 1 - (T_{A_d} + T_{A_w}) . \quad (11)$$

Strictly speaking, in this way only absorption of solar radiation by hygroscopic particles is considered; absorption by dry aerosols is neglected.

Carbon Dioxide. The transmittance is estimated according to Burch et al. (1960):

$$T_{CO_2} = 1 - 1.35* 10^{-3} (U_{CO_2} + 0.0129)^{0.26} - 7.5* 10^{-4} . \quad (12)$$

Oxygen. Yamamoto (1962) gives the transmittance function as

$$T_{O_2} = 1 - 7.5* 10^{-3}* (m*)^{0.875} . \quad (13)$$

3.2.2 Estimation of β, Zenith Angle, and I_o

The ratios of forward-scattered to total scattered radiation values used are those of Robinson (1962) (fig. 2). Since monthly data are used in the study it is imperative that an appropriate mean value of zenith angle be used for each month. The mean zenith angle values were derived as follows.

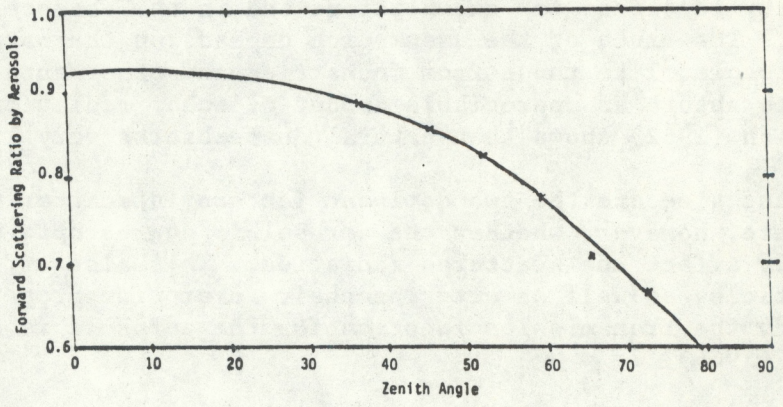

Figure 2.--Forward scattering ratio vs. zenith angle.

The amount of daily solar radiation for a horizontal surface at the top of the atmosphere is given by

$$I_o = \frac{S_o}{r^2} * 6.9375 * 10^{-4} * H^* * \cos \bar{z} \quad \text{(in W m}^{-2}\text{)} \tag{14}$$

(note S_o in W m^{-2}). Also, I_o can be written (Sellers, 1965)

$$I_o = \frac{S_o}{r^2}\ 6.9375 * 10^{-4} * H^* * (\frac{H}{2} * \sin \Theta * \sin \delta + \cos \Theta \cos \delta \sin \frac{H}{2}) \quad \text{(in W m}^{-2}\text{)} . \tag{15}$$

Thus,

$$\cos \bar{z} = (\frac{H}{2} \sin \Theta \sin \delta + \cos \Theta \cos \delta \sin (\frac{H}{2})) . \tag{16}$$

In the above two equations it should be noted that the first H/2 in each equation is in radians, but the second H/2 (the sine expression) is in degrees.

Monthly mean values of r^2, δ, and H were taken from List (1971). Solar radiation fluxes for a horizontal surface at the top of the atmosphere for a given latitude and month of the year were calculated from equation 15. From equation 16, air mass mean values were calculated by

$$M = 1/\cos \bar{z} . \tag{17}$$

3.2.3 Cloudless Sky Components

The direct beam reaching the horizontal surface of the earth in cloudless sky is given by

$$I = I_0 \cos \bar{z}\ T_{W_a}\ T_{W_s}\ T_{O_3}\ T_{O_2}\ T_{CO_2}\ T_{R_s}\ T_{A_a}\ T_{A_s} . \tag{18}$$

In this study T_{W_s} is included in T_{R_s}, and T_{A_a} is assumed to be equal to one.

The equation for diffuse radiation component is given by Davies et al. (1975) (with carbon dioxide and oxygen transmittances added):

$$D = I_0 \cos \bar{z}\ T_{O_3}\ T_{O_2}\ T_{CO_2}\ T_{W_a}\ T_{A_s}\ [1-T_{R_s}]\ \beta . \tag{19}$$

Assuming that absorption precedes scattering and that absorption by water vapor attenuates only the direct beam (Robinson, 1958, 1962; Paltridge and Platt, 1976), diffuse radiation components can be divided into that which results from Rayleigh scattering,

$$S_R = I_0 \cos \bar{z}\, T_{O_3}\, T_{O_2}\, T_{CO_2}\, T_{W_a}\, (1-T_{R_s})\, T_{A_s}\, \beta\ , \tag{20}$$

and that which results from aerosol scattering,

$$S_a = I_0 \cos \bar{z}\, [T_{O_3}\, T_{O_2}\, T_{CO_2}\, T_R - (1-T_{W_a})]\, [1-T_{A_a}\, T_{A_s}]\, \omega_o\, \beta\ . \tag{21}$$

It should be noted that in equation 21, the multiplicative property is not extended to the water transmission function. This is because, in the infrared region where aerosol scattering is in force, the band model arrays are no longer big enough, a necessary condition for the multiplicative property (Goody, 1964).

As the primary diffuse radiation hits the earth's surface, secondary and higher multiply-reflected diffuse components are generated. The magnitude strongly depends on the surface and atmospheric albedos. Rasool and Schneider (1971) have parameterized the secondary reflection component as

$$D_M = \alpha_s\, \alpha_a\, (I + S_R + S_a)/(1 - \alpha_a\, \alpha_s)\ . \tag{22}$$

Thus total diffuse radiation in cloudless skies can be written as

$$D = S_R + S_a + D_M\ . \tag{23}$$

3.2.4 Cloudy Skies: Direct and Diffuse Solar Radiation Components

In order to minimize the errors encountered through the use of either cloud data or sunshine data separately, a coefficient E_c, employing data on both clouds and sunshine hours (sometimes referred to as effective cloudiness), is used (Hoyt, 1977). The definition of Kondratyev (1969) is adopted:

$$E_c = [(1 - n/N + CA)/2]\ . \tag{24}$$

The direct and diffuse solar radiation components are respectively given as

$$I_c = I * (1 - E_c) \tag{25}$$

and

$$D_c = D * (1 - CA) + E_c * \eta * (I + D)\ . \tag{26}$$

As mentioned earlier, η had to be estimated for each grid point, since a value of one for a given latitudinal band proved to be inadequate. The method used was that described by Albrecht (1955). The seasonal empirical formulas for January, April, July, and October, based on data from the ten selected stations, are

$$\eta(1) = 0.86 - 1.30*\sin\theta - 0.87*C_r + 1.31*\sin\theta * C_r, \tag{27}$$
$$\eta(4) = 0.86 - 1.29*\sin\theta - 0.83*C_r + 1.24*\sin\theta * C_r, \tag{28}$$
$$\eta(7) = 0.86 - 1.36*\sin\theta - 0.86*C_r + 1.35*\sin\theta * C_r, \tag{29}$$
$$\eta(10) = 0.81 - 1.28*\sin\theta - 0.84*C_r + 1.33*\sin\theta * C_r. \tag{30}$$

The above formulas are based on the assumption that S + CA = 1. However, a preliminary analysis of this quantity in the present study indicated that deviations of about 20% were possible. Attempts were made to overcome this problem through correction to S and CA as follows:

$$\eta \text{ correction} = (\Delta * \eta)/(\eta + CA), \tag{31}$$

$$CA \text{ correction} = (\Delta * CA)/CA + \eta). \tag{32}$$

From 25 and 26 the global solar radiation for cloudy atmosphere is given by

$$G_c = I_c + D_c. \tag{33}$$

The above approach assumes a one-layer cloud model, which, in many aspects, may not be representative. However, the higher orders of multiple reflection and scattering rapidly decline, as shown by values from equation (9). Hence, this model is likely to be sufficiently accurate for monthly mean values.

4. PERFORMANCE OF THE METHODS

An absolute comparison of the estimated and observed values is meaningless since in many cases quality control has not been performed for the global solar radiation data observed in Africa. However, if we make a basic assumption that whatever kinds of errors exist in observed data are consistent rather than seasonal, we can select statistics that will reveal some seasonal variations in estimated and observed solar radiation values. It should be pointed out that in the present analysis only data for January, April, July, and October will be discussed, since these are the only complete sets of data.

The following quantities were calculated for both the estimated and the observed sets of global solar radiation data in order to compare the two.

(i) Annual variability:

$$A_{v_1} = (X_i - \bar{X})/\bar{X} \quad (\%)$$

where X_i is for estimated or observed monthly mean solar radiation for a particular station, i runs from 1 to 12, and $\bar{X}$ is the annual mean for the same set.

(ii) Annual variability (with respect to observed values):

$$A_{v_2} = (X_{E_i} - \bar{X}_s)/\bar{X}_s \quad (\%)$$

where E_i stands for estimated and s stands for observed.

(iii) Standard deviation:

$$S = (\Sigma(X_i - \bar{X})^2/12)^{\frac{1}{2}} .$$

(iv) Root mean square error:

$$r_{ms} = (\Sigma(X_{S_i} - X_{E_i})^2/12)^{\frac{1}{2}} .$$

(v) Deviation of estimates from observed:

$$d_e = (X_{S_i} - X_{E_i})/X_{S_i} \quad (\%) .$$

(vi) Coefficient of variability:

$$r = S_i / \bar{X}_i .$$

Caution must be exercised when examining group (v) since no quality control has been performed on the measured radiation values. The absolute meaning of the values may be misleading. Deviations of estimated from observed values are shown in figs. 3 and 4 and table 2. Inspection of the standard error of estimate reveals that the ST method is substantially better than the R method and that ST-CS is better than ST-C. The same conclusion may be drawn from the percentage deviation of estimates from observed. Examination of the coefficient of variability also points to the same conclusion. Except for Nairobi in July and Port Sudan in January, the deviation of estimated from observed values at each station is 10% or less. This figure should be used with caution because the absolute values of some of the observed data are uncertain.

On the basis of standard deviation both models seem to perform equally well, so it is difficult to use that as a way of differentiating between them. From fig. 4 one finds that, in general, the annual variations of observed and estimated solar radiation values are similar, that is, the curve of the estimated values closely matches that of the observed values. Except for some minor disagreements in amplitudes for Kinshasa and Nairobi, the estimated annual variability is close to the observed at all 10 stations. Figure 4b shows monthly deviation of estimates from observed values at Port Sudan, Pretoria, Nairobi, and Kinshasa for the whole year to give some idea of the performance for months other than the four selected ones in fig. 4a. The results for Kinshasa and Pretoria are particularly encouraging.

The discrepancies at Nairobi (particularly in July) may be attributed to the presence of a low-level inversion during most of the period. Presumably the satellite is unable to differentiate between low-level clouds and the ground or, if it can, the difference is lost in the averaging, since this may be a localized phenomenon and the satellite data have low spatial resolution. Furthermore, the layers with high water vapor content are too low to be included in the first significant level quoted in the climatological data. Port Sudan, on the other hand, although also influenced by the spatial resolution problem, has a high surface albedo, which may interfere with the cloud measurements.

Further evidence for the accuracy of the models is shown in figs. 5 through 7, where plots of observed vs. estimated global solar radiation values show good agreement. The ST-CS approach once again appears to be superior.

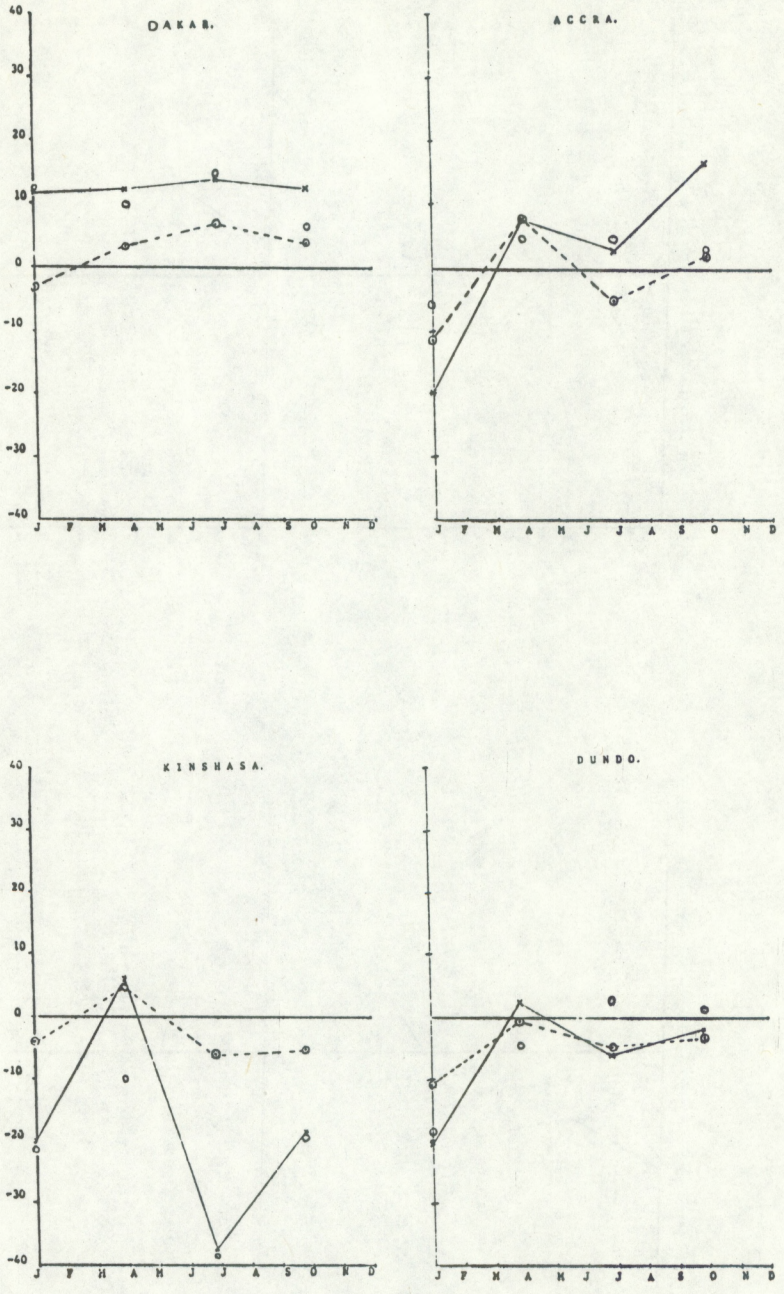

Figure 3.--Deviation (%) of estimated from observed values of solar radiation at the 10 stations where observations were made (X: R method, O: ST-C method, θ: ST-CS method).

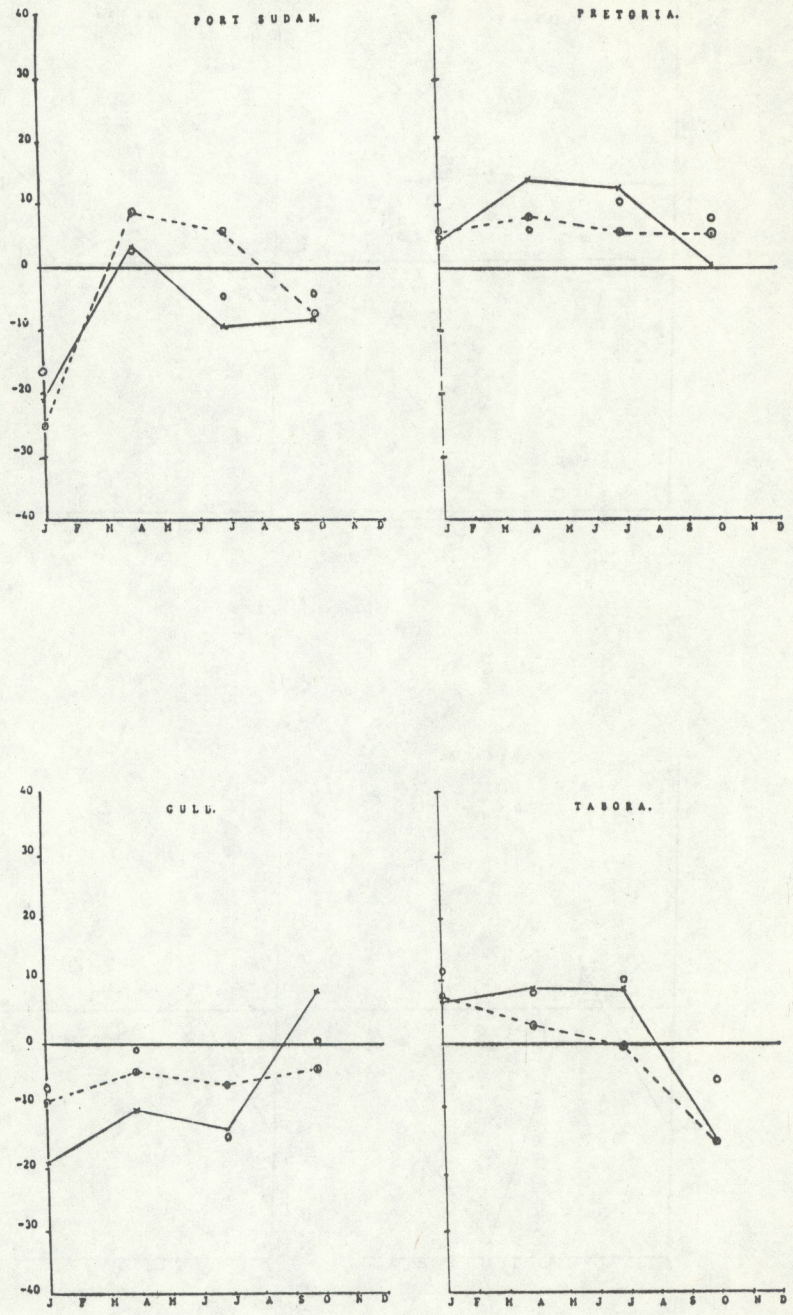

Figure 3.--Continued.

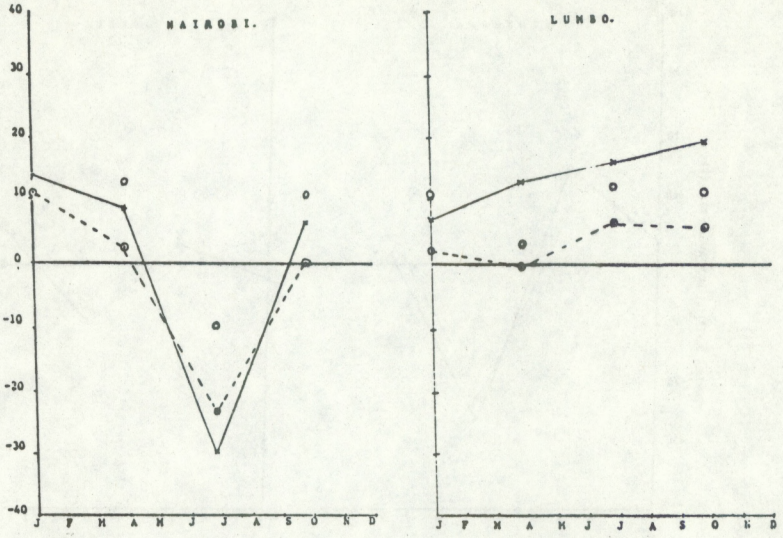

Figure 3.--Continued.

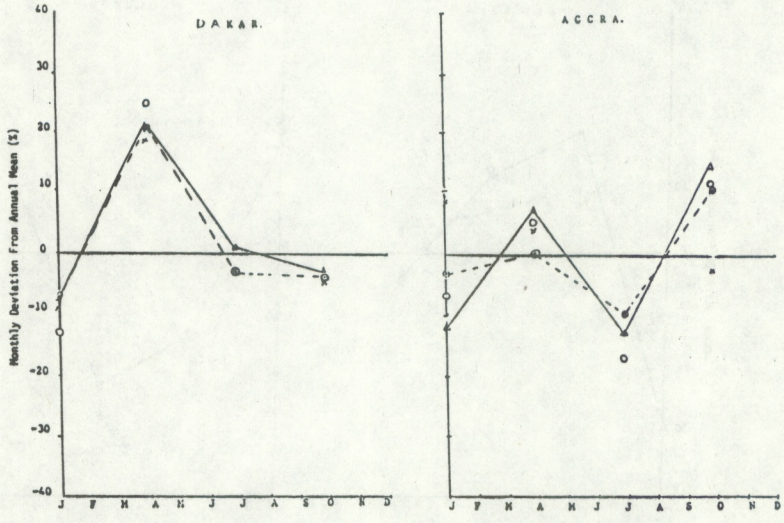

Figure 4a.--Monthly deviation (%) of observed and estimated solar radiation from annual mean for January, April, July, and October (Δ: Observed, X: R method, O: ST-C method, Θ: ST-CS method).

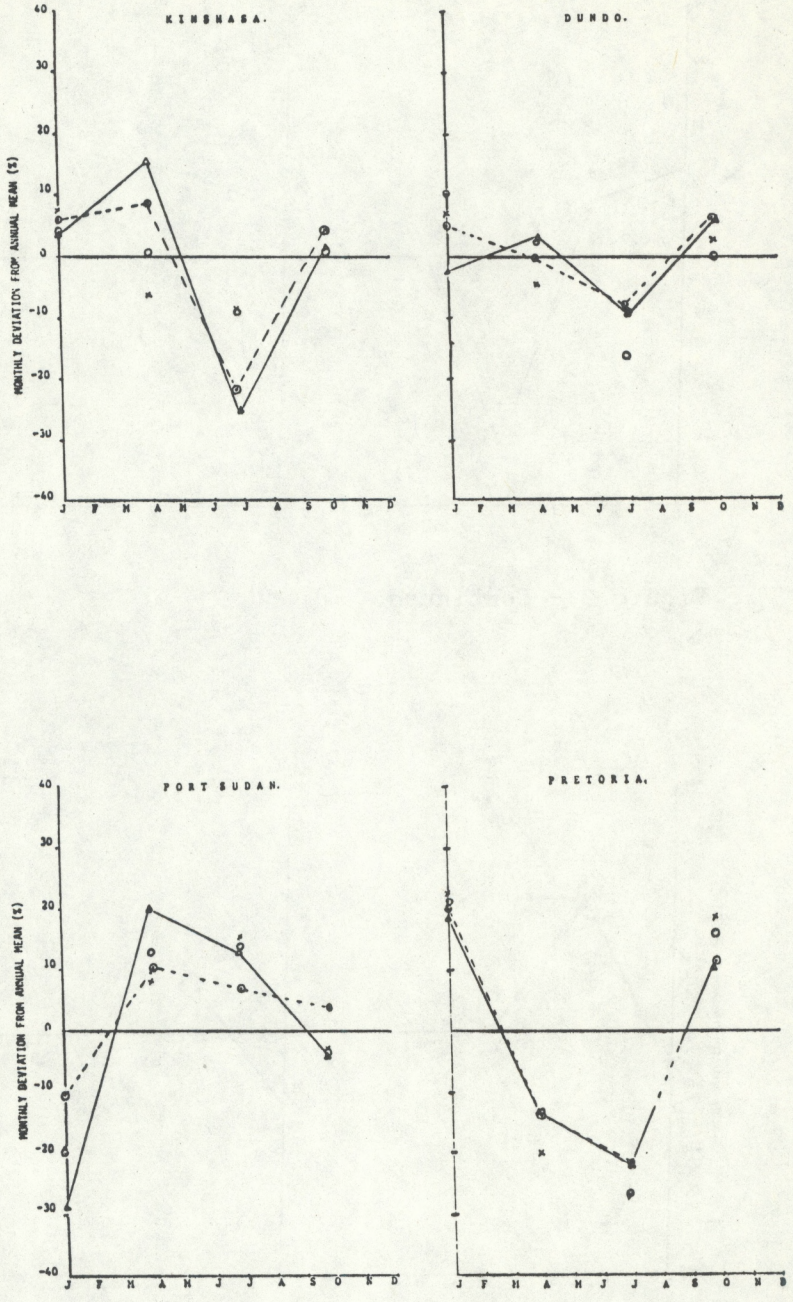

Figure 4a.--Continued.

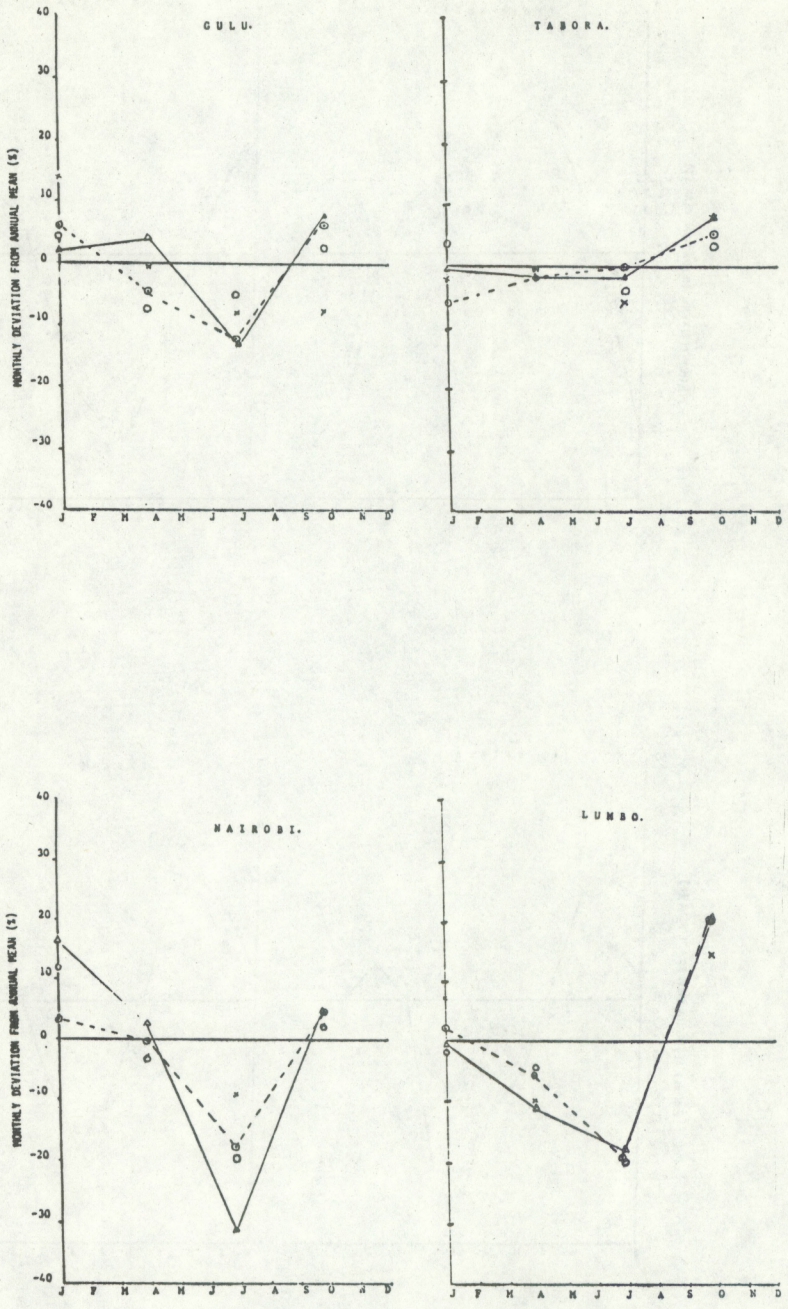

Figure 4a.--Continued.

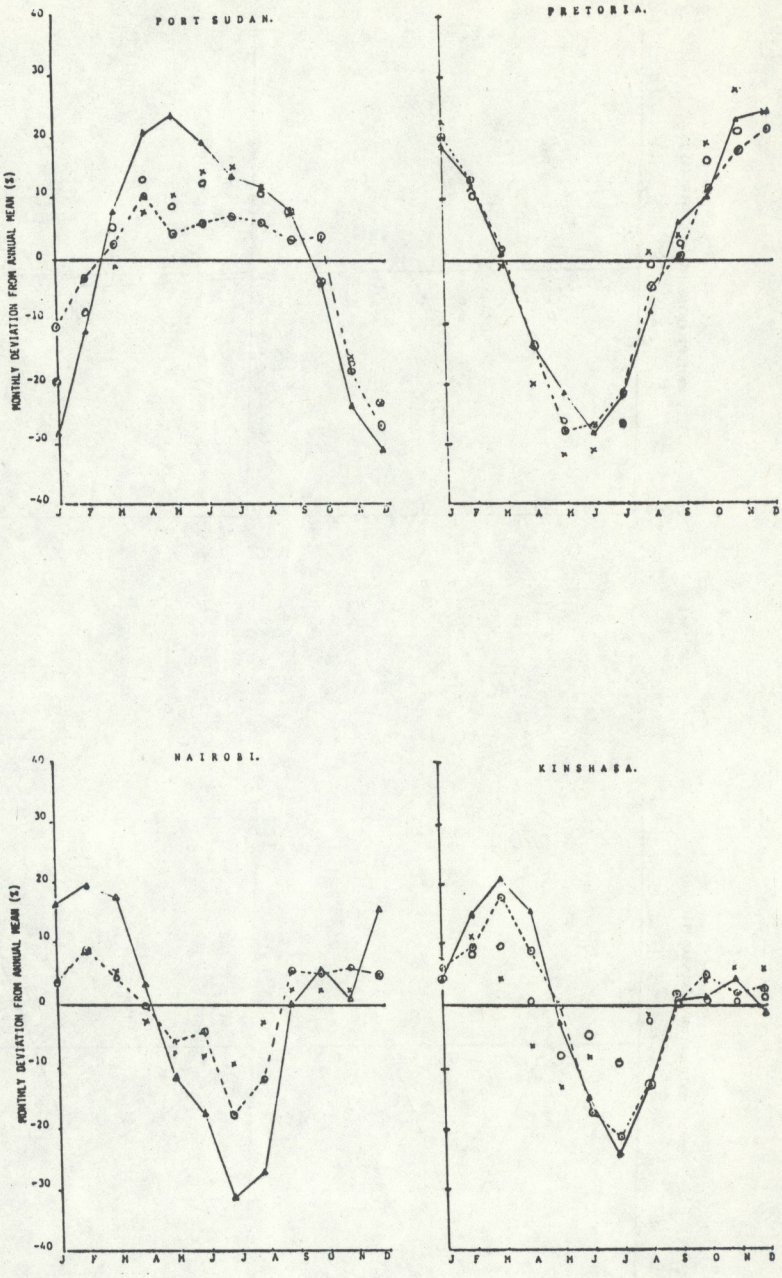

Figure 4b.--Monthly deviation (%) of observed and estimated solar radiation from annual mean for all 12 months (Δ: Observed, X: R method, O: ST-C method, Θ: ST-CS method).

Table 2.--Statistics for estimated and observed solar radiation values

Station	Root Mean Square Error			Standard Deviation				Variability				Mean Annual Solar Radiation (W m ^{2})			
	R	ST-C	ST-CS	R	ST-C	ST-CS	OBSER.	R	ST-C	ST-CS	OBSER.	OBSER.	ST-C	ST-CS	R
Dakar	33	25	19	20	26	22	30	.09	.12	.09	.12	239	215	230	217
Accra	26	16	20	19	20	15	24	.09	.10	.07	.12	207	203	212	213
Kinshasa	33	39	20	15	12	20	23	.08	.06	.11	.13	172	185	225	212
Dundo	20	21	6	14	20	17	11	.07	.10	.08	.06	192	210	217	216
Port Sudan	23	17	19	35	33	20	46	.14	.13	.08	.19	239	211	281	252
Pretoria	20	16	29	46	41	38	41	.22	.19	.18	.18	229	255	231	215
Gulu	25	15	20	21	9	15	15	.09	.04	.07	.07	207	232	226	235
Tabora	21	23	14	12	7	11	10	.05	.03	.05	.04	224	212	213	232
Nairobi	29	25	16	13	24	18	39	.06	.11	.08	.17	226	235	216	232
Lumbo	34	24	24	27	28	32	34	.13	.13	.14	.15	233	228	213	209

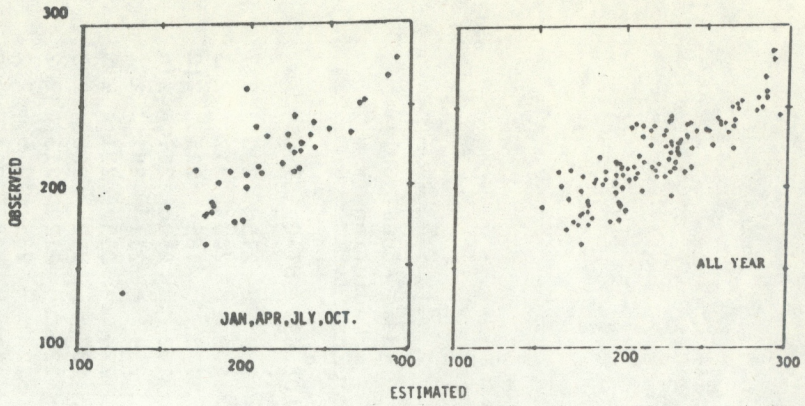

Figure 5.--Comparison of estimated (ST-CS method) and observed global solar radiation in W m^{-2}.

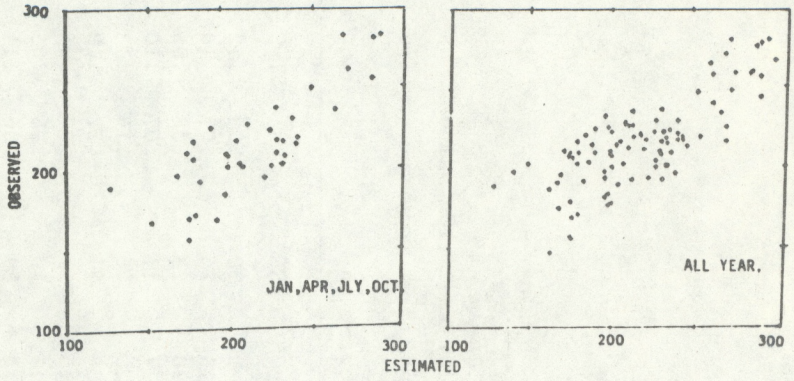

Figure 6.--Comparison of estimated (ST-C method) and observed global solar radiation in W m^{-2}.

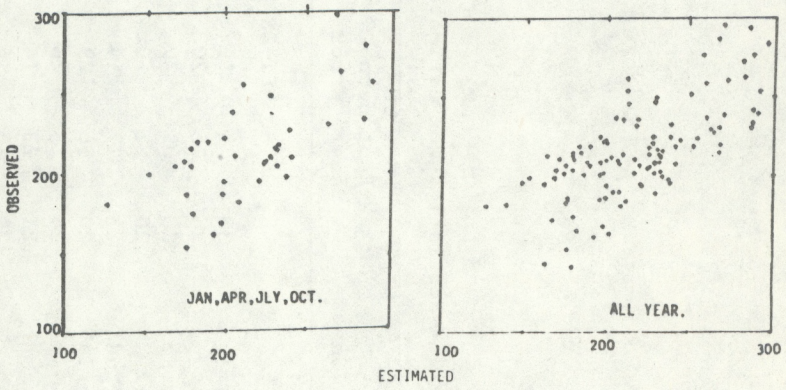

Figure 7.--Comparison of estimated (R method) and observed global solar radiation in W m^{-2}.

5. COMPARISON WITH OTHER STUDIES

Budyko (1974) gives climatological solar radiation distributions for the continent of Africa for June and December over a period of several years. Comparison with this study's distributions shows, in general, a large number of similarities. The absolute values, however, differ, and in some cases by substantial amounts. For June and December, Budyko's southern high cells have values of 220 and 340 W m^{-2}, respectively, compared with 200-220 and 260-300 W m^{-2}, respectively, for the present study. The northern high cell values are also in the same range: 220 and 350 W m^{-2} for June and December, respectively, in Budyko and 280 and about 250 W m^{-2}, respectively, in the present study. The southwest Africa and adjoining Congo Basin regions have relatively deeper low centers in Budyko than in the present study. Values for June and December are 130 and 160 W m^{-2}, respectively, in Budyko's work and 160-180 and 180-210 W m^{-2}, respectively, in the present study.

Comparison between estimated global solar radiation values from this study and from that of Mani (1976) reveals many similarities for January, April, July, and October. Concentrating on the ST-CS method, the major discrepancies are in the April, July, and October northern high center cells. In absolute values, magnitudes differ by about 30 to 60 W m^{-2}. Elsewhere, except for southwest Africa and the Congo Basin, where low center values differ by about 60 W m^{-2} for April, the low and high center cells generally differ by about 10 W m^{-2}.

The main source of discrepancies between the present study and those of Budyko and Mani is the network coverage. In Budyko's study, the total number of stations for the whole world (on land only) was 2100. Considering the time of publication, there could not have been much coverage of Africa. In Mani's work, the network coverage is again sparse. Hence, in both studies there was heavy reliance on extrapolation. With the tropical systems this could lead to large errors.

This, however, does not imply that the present work is error-free. There is, for example, a marked failure to simulate seasonal amplitude variations of solar radiation for some stations near the equator. This has been attributed to the data sample not being large enough to form statistically stable seasonal samples. While this may apply to the R method, it fails to account for the ST-CS method discrepancies. Another possible error source is the resolution in the satellite data, which may also contribute a significant error.

Overall, the results of the studies, especially Mani's and the present study, have more similarities than discrepancies.

6. CONCLUSION

The monthly distributions of global solar radiation values derived from either model for the continent of Africa give meaningful climatological data sets, that is, the estimates are reliable, as exhibited by the basic statistics from the ten selected stations. A finer-resolution satellite data set would probably improve the estimates. They might be better still if satellite cloud and solar radiation values were taken simultaneously and regressed. In all, the discrepancies between the results gained by different methods are very much

outweighed by the agreements, demonstrating further that satellite data can be of great use in solar radiation climatology. The methods are also useful for application to solar energy problems.

7. ACKNOWLEDGMENTS

The author wishes to express his sincere gratitude to Dr. Kirby Hanson and Dr. John Hay for their stimulating discussions and suggestions during this study. The research was supported in part by NSF grant number ATM-7815529 and NOAA's Geophysical Monitoring for Climatic Change Program.

8. REFERENCES

Albrecht, F. H. W. (1955): Methods of computing global radiation. Geofis. Pura Appl. 32:131-138.

Angström, A. (1924): Solar and terrestrial radiation. Q. J. R. Meteorol. Soc. 50:121-125.

Baker, D. G., and D. A. Haines (1969): Solar radiation and sunshine duration relationships in the North-Central Region and Alaska: basic computation. North Central Regional Research Publication 195, Tech. Bull. 262, Agricultural Experiment Station, State of Minnesota, St. Paul, Minn.

Budyko, M. I. (1974): Climate and Man. Academic, New York.

Burch, D. E., D. Gryvanak, and D. Williams (1960): The infrared absorption by CO_2. Report on Project 778, Ohio State University Research Foundation, Columbus, Ohio.

Davies, J. A., W. Schertzer, and M. Nunez (1975): Estimating global solar radiation. Boundary Layer Meteorol. 9:33-52.

Goody, R. M. (1964): Atmospheric radiation. Sec. 4. Oxford Univ. at Clarendon Press, London.

Hanson, K. J. (1976): A new estimate of solar irradiance at the Earth's surface on zonal and global scales. J. Geophys. Res. 81:4435-4453.

Hoyt, D. V. (1976): The radiation and energy budgets of the Earth using both ground-based and satellite-derived values of total cloud cover. NOAA Tech Report ERL 362-ARL 4, NOAA/ERL, Boulder, Colo.

Hoyt, D. V. (1977): Percent of possible sunshine and the total cloud cover. Mon. Weather Rev. 105:648-652.

Katayama, A. (1966): On the radiation budget of the troposphere over the Northern Hemisphere (1). J. Meteorol. Soc. Japan 44:381-401.

Kondratyev, K. (1969): Radiation in the Atmosphere, Chapters 5 and 6. Academic, New York.

Kondratyev, K. (1973): Radiation Characteristics of the Atmosphere and Earth's Surface, Chapters 6 and 7. NASA TTF-678, published for NASA and NSF by Amerind Ltd., New Delhi.

Lacis, A. A., and J. E. Hansen (1974): A parameterization for the absorption of solar radiation in the Earth's atmosphere. J. Appl. Sci. 31:118-132.

List, R. (1971): Smithsonian Meteorological Tables. Smithsonian Institution Press, Washington, D.C.

Mani, A. (1976): Radiation measurements for solar energy applications. Proceedings of the UNESCO/WMO Symposium, Geneva, 30 Aug.-3 Sept. 1976. WMO No. 477, 125-143, World Meteorological Organization, Geneva.

Paltridge, G. W., and C. M. R. Platt (1976): Radiation processes in meteorology and climatology. Elsevier, New York, 89-140.

Pearman, G. I. (1978): Atmospheric carbon dioxide: recent advances in monitoring and research. In Climatic Change and Variability--A Southern Perspective. A. B. Pittock, L. A. Frakes, D. Jenssen, J. A. Peterson, and J. W. Zillman (eds.), Cambridge Univ. Press, New Rochelle, N.Y., 282-293.

Rasool, S. I., and S. H. Schneider (1971): Atmospheric carbon dioxide and aerosols effect of large increases on global climate. Science 173:138-141.

Robinson, G. D. (1958): Some observations from aircraft of surface albedo and absorption of cloud. Arch. Meteorol. Geophys. Bioklimatol. B9:28-41.

Robinson, G. D. (1962): Absorption of solar radiation by atmospheric aerosols as revealed by measurements from the ground. Arch. Meteorol. Geophys. Bioklimatol. B12:19-40.

Rockwood, A. A., and S. K. Cox (1978): Satellite inferred surface albedo over northwestern Africa. J. Atmos. Sci. 35:513-522.

Sadler, J. C. (1968): Average Cloudiness in the Tropics from Satellite Observations. East-West Centre Press, Honolulu, Hawaii.

Sasamori, T., J. London, and D. V. Hoyt (1972): Radiation Budget of the Southern Hemisphere. Meteorological Monographs, Vol. 13, No. 35, American Meteorological Society, Boston, Mass.

Sellers, W. D. (1965): Physical Climatology. University of Chicago Press, Chicago, Ill., 16.

Suckling, P. W., and J. E. Hay (1977): A cloud layer-sunshine model for estimating direct, diffuse and total solar radiation. Atmosphere 15:194-217.

U.S. Department of Commerce (1965-1972): Monthly Climatic Data. Washington, D.C.

Van de Boogaard, H. (1977): The mean circulation of the tropical and subtropical atmosphere. Atmospheric Analysis and Prediction Division, National Center for Atmospheric Research, Boulder, Colo.

Yamamoto, G. (1962): Direct absorption of solar radiation by atmospheric water vapor, carbon dioxide and molecular oxygen. J. Atmos. Sci. 19:182-188.

Appendix

GENERAL CLIMATOLOGICAL FEATURES OF AFRICA

To fully appreciate the relationships between solar radiation components and atmospheric synoptic systems, one should be familiar with the prevalent air mass flows and related pressure fields. The situation is summarized by the streamlines for January and July shown in fig. 8 (Van de Boogaard, 1977; H. Van De Boogaard, NCAR, Boulder, Colo., personal communication, 1979). Conditions that may influence global solar distribution are described below.

During January, the air flow over the northern part of the continent is controlled by two subtropical anticyclones. One is centered about latitude 30° N and longitude 20° E and another one about latitude 35° N and longitude 10° W. These anticyclones give rise to predominantly northeasterly winds, which may penetrate further south even beyond the equator. These winds are dry since they have a long trajectory over land. To the south, anticyclones are more extensive laterally. The south Atlantic anticyclone is located about longitude 10° W and latitude 30° S. The south Indian Ocean anticyclone center is at the same latitude, but the longitude is about 75° E. It, however, has a ridge extending westward almost to the edge of the southeastern tip of the continent. The southern part of the continent is under relatively low pressure. To the west the southeasterlies from the south Atlantic anticyclone become southwesterlies to westerlies as they turn into the relatively low pressure region over the continent. These winds are moist and hence are rain-bearing winds. On the southeastern side of the continent, south easterlies tend to easterlies, and after traversing much of the Indian Ocean they are heavily loaded with moisture. North of about 10° latitude the flow is mainly from the northeast. The Intertropical Convergence Zone (ITCZ), the meeting zone of the northern and southern wind regime, is illustrated in fig. 8A. In a way the ITCZ marks the northern limit of active weather during this time.

In July, the systems described above are still the dominant ones except that they are all displaced north. To the south the anticyclonic centers occupy the same positions apart from a slight westward movement for the Indian Ocean center and a general intensification of pressure over much of the southern area. Over the southern sector of the continent southerly winds dominate and penetrate deep into the Northern Hemisphere thermal low, the ITCZ, stretching across the continent between latitudes 10° and 20° N. North of the thermal low, northerly winds prevail. To the northeast, the January Arabian anticyclones have given way to a low pressure area, and much of the flow from the Indian Ocean anticyclone turns into this low pressure area. Over the continent around the equator and about 30° E another relatively low pressure area exists. This, together with the Arabian low pressure area, gives rise to a diffluent flow over the east coastal areas of the continent. Weather activities are mainly north of 10° S latitude and most pronounced over west Africa because of the intensification of the west African monsoon.

Of interest in solar radiation studies is the realization of moisture distribution in synoptic systems; air-flow characteristics and trajectories such as these will determine the distribution of optically active atmospheric constituents. The January and July cases relate to the extreme southward and northward limits of synoptic systems that control the airflow. The cases of other months lie between these extremes.

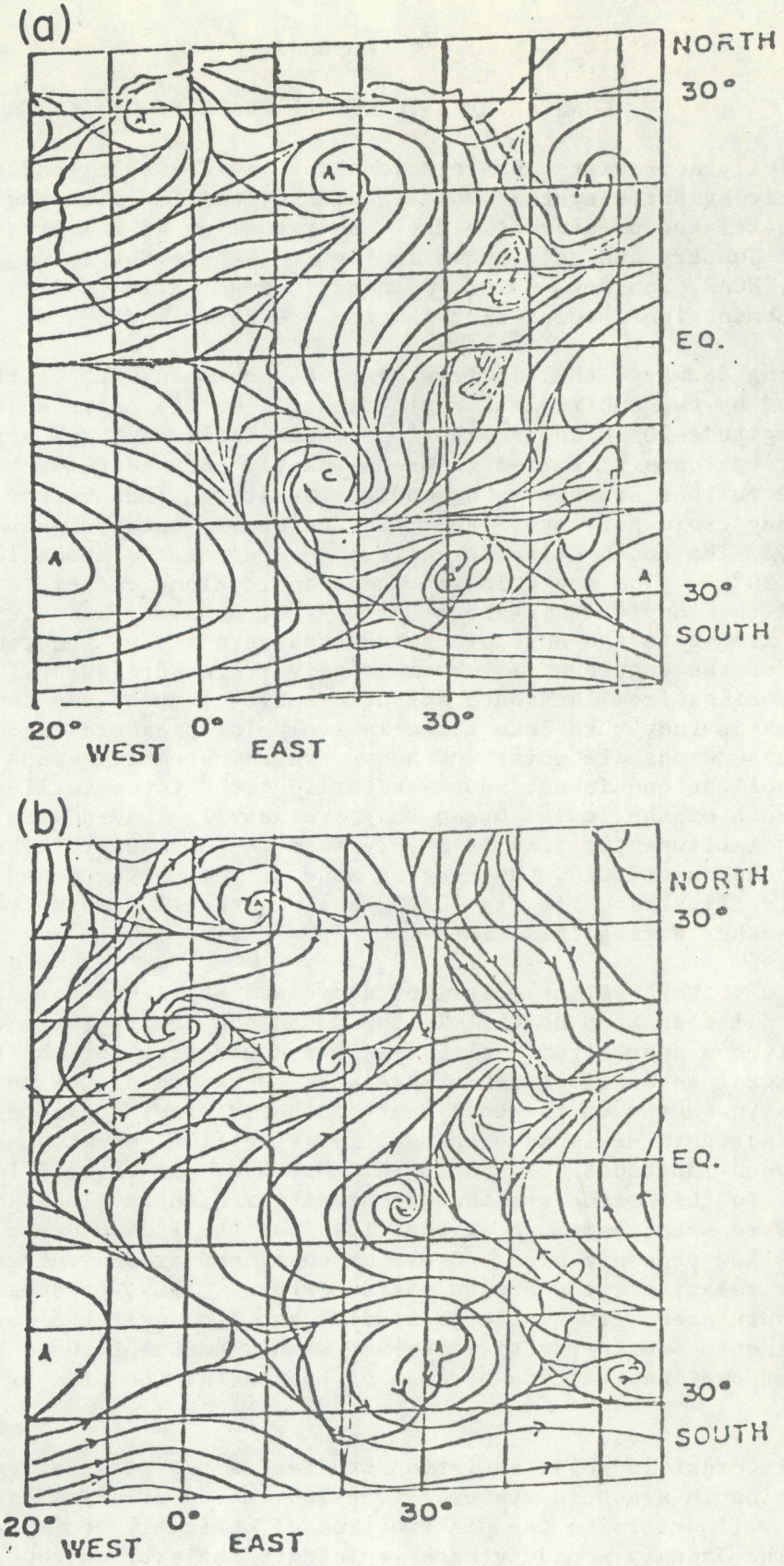

Figure 8.--Mean streamlines at 850-mb level (1961-1974): a) January, b) July.

Figures 9 through 13 give the distributions of global solar radiation over the continent of Africa. Focusing our attention on January, April, July, and October, we observe that both ST and R method estimates have the same major features. The R method gives higher values of magnitude in the north and lower in the south of the continent for January. The effects of the persistent atmospheric synoptic systems on the solar radiation estimates are quite distinct. Major factors are the movements of ITCZ and the cyclones and anticyclones in the various seasons. The main features for January, April, July, and October are as follows:

(i) January. During this period the ITCZ is situated south of the equator, and the associated cloud cover stands out in low global solar radiation values stretching obliquely across the continent between about latitude 5° S to the west and 15° S to the east with values averaging below 200 W m^{-2}. North and south of this low radiation belt, values rise to a high of about 250 W m^{-2} centered about 5° N and to about 260 W m^{-2} centered about 25° S.

(ii) April. Compared with the January case, there is a northward and eastward movement of the seasonal atmospheric synoptic system. This leaves the south section of the continent still experiencing wind confluence. The coupling of the sun's northward movement and the heavy moisture in the south reduces the southern solar radiation values. The northern global solar radiation values increase. A high of 280 W m^{-2} is centered at about latitude 10° N. To the south the 280 W m^{-2} region gives way to about 160-180 W m^{-2}. Solar radiation patterns tend to show that eastern parts of the continent receive higher global solar radiation than the western parts. This may be a result of the high land in the east deflecting the moisture-laden air, leaving the west with relatively dry air, which would lead to less cloud formation and less absorption of solar energy.

(iii) July. At this time of year, the ITCZ has moved farthest north. Associated low global solar radiation values are centered about latitude 5° N. The monsoon-type system flow of west Africa accentuates the ITCZ effects; to the east the extension southward of a ridge from the Arabia high dilutes the ITCZ effects. Solar radiation for much of the continent north of latitude 15° N is greater than 220 W m^{-2}. The southern high, barely discernible in the R and ST-C methods, except as a protrusion from the northern high region, averages just over 180 W m^{-2} and is centered about 10° S. Farther south, values decrease to 100-120 W m^{-2}.

(iv) October. During this period major atmospheric systems drift southward. The southern high radiation value builds to more than 260 W m^{-2} and is centered about latitude 20° S. The northern high radiation value reduces, but not at the same rate that the southern radiation values are building up; it stands at slightly more than 240 W m^{-2} and centers at 10° N latitude. Again, the values over the eastern side of the continent are higher than those in the same latitude over the western side.

In general, the northern portion of the continent shows less variability than the comparable latitude band in the southern portion. This may be a result of the differences in ocean and land distribution between the two hemispheres.

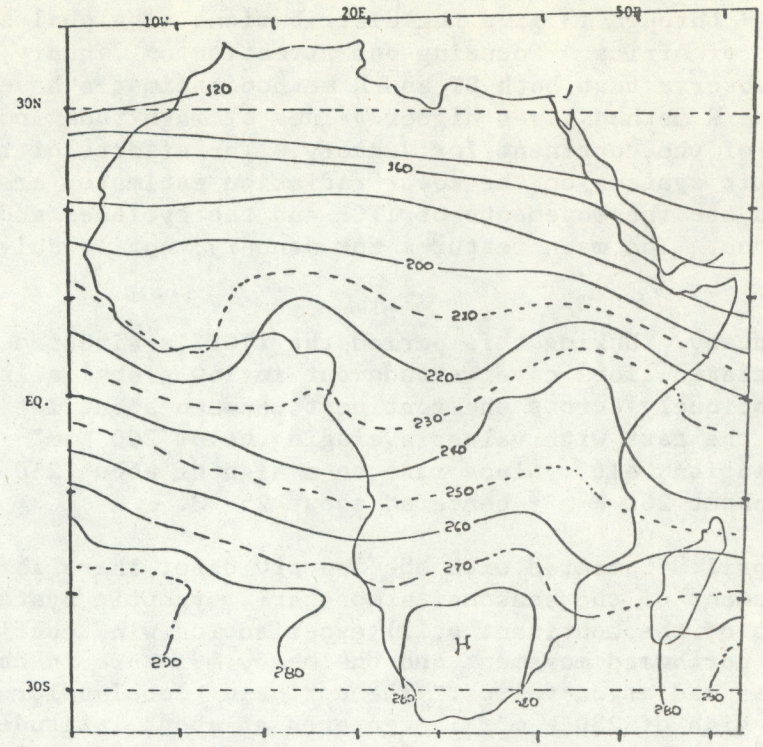

Figure 9.--Direct solar radiation on a horizontal surface (W m^{-2}): (a) January.

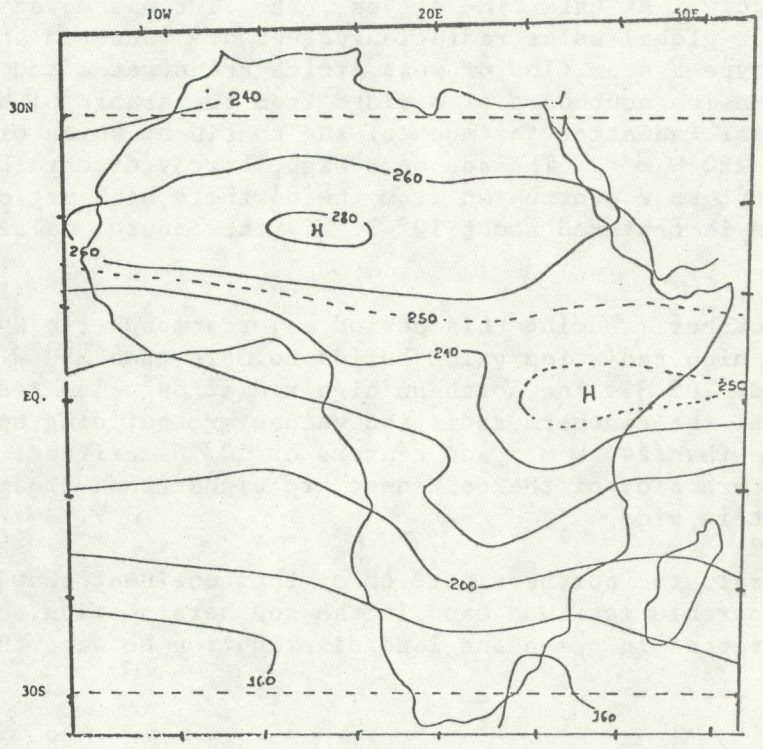

Figure 9b.--April.

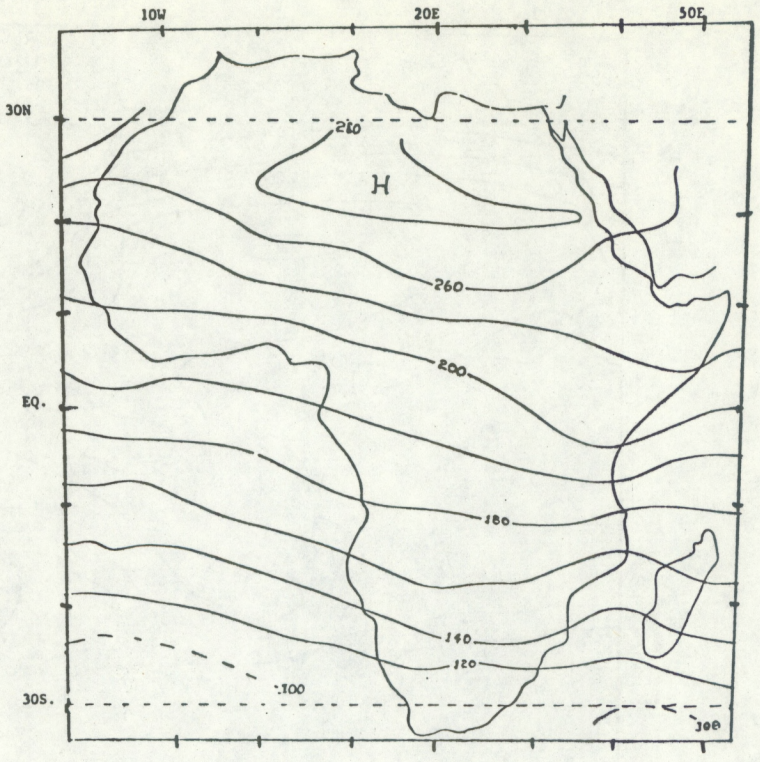

Figure 9c.--July.

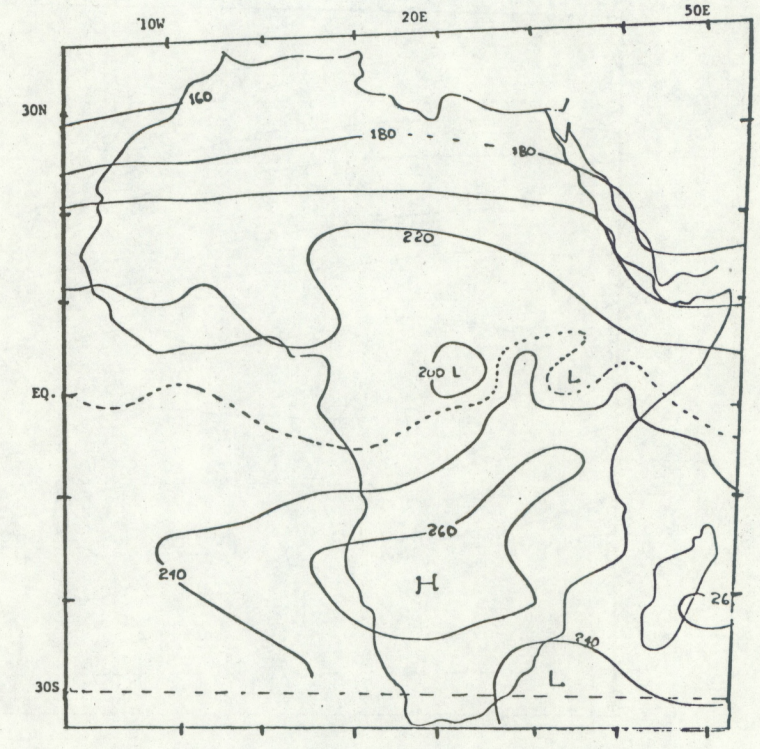

Figure 9d.--October.

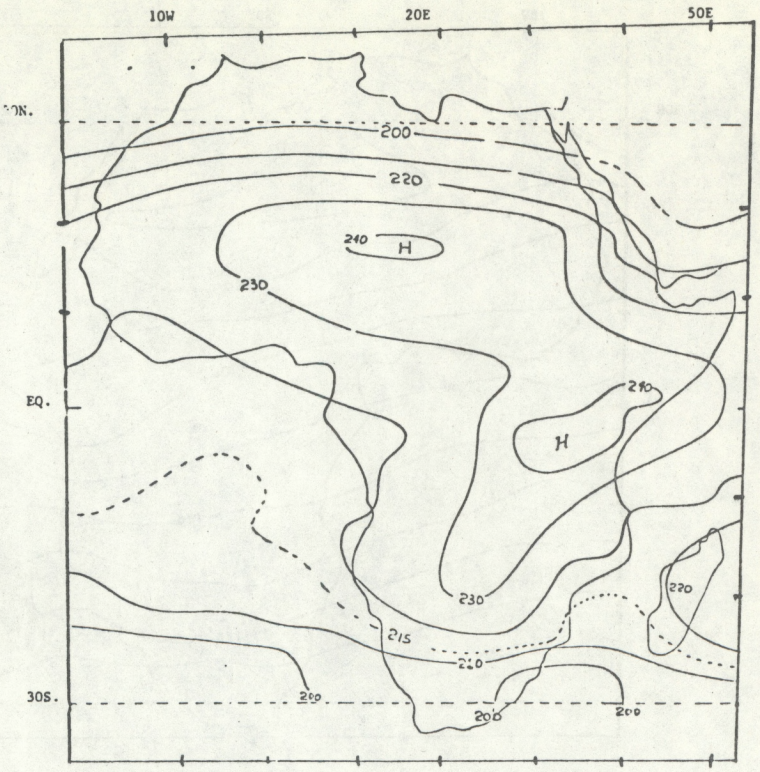

Figure 9e.--Annual.

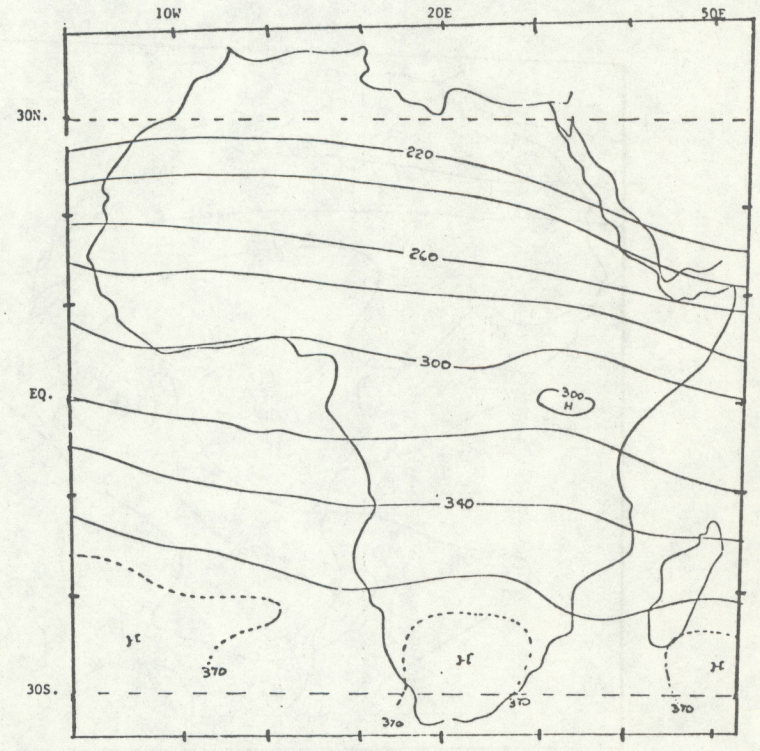

Figure 10.--Global clear sky solar radiation on a horizontal surface ($W\ m^{-2}$): (a) January.

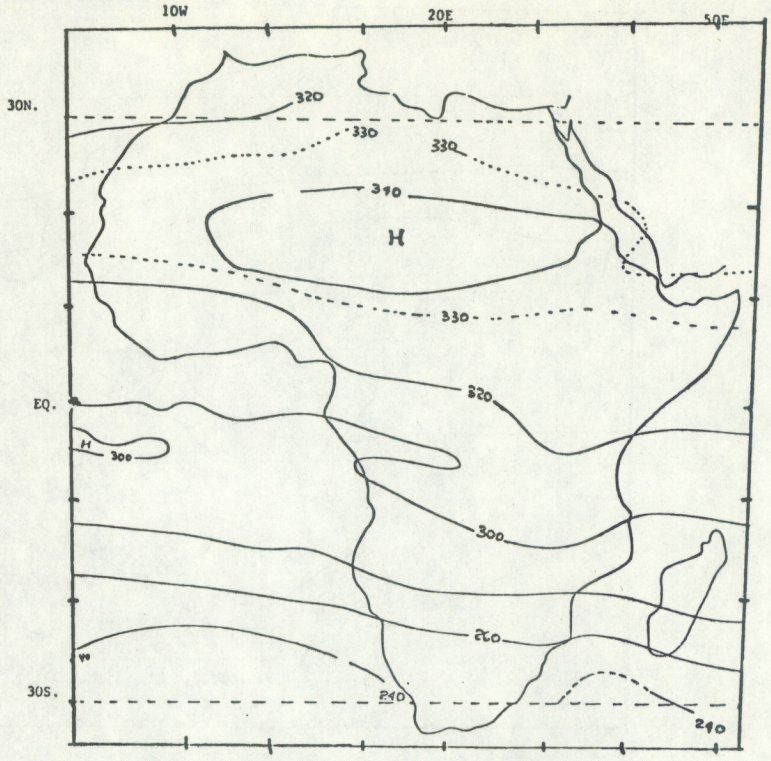

Figure 10b.--April.

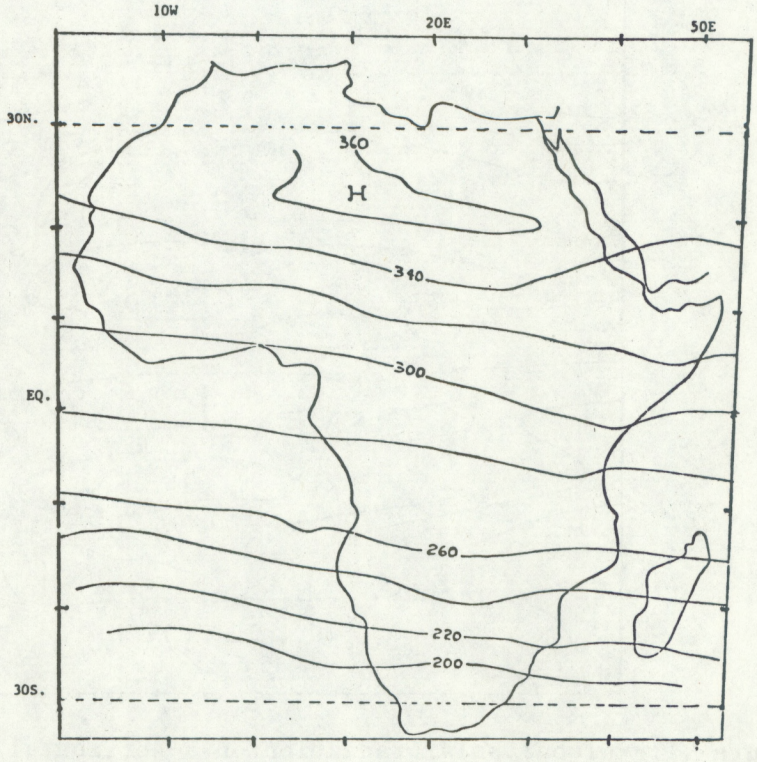

Figure 10c.--July.

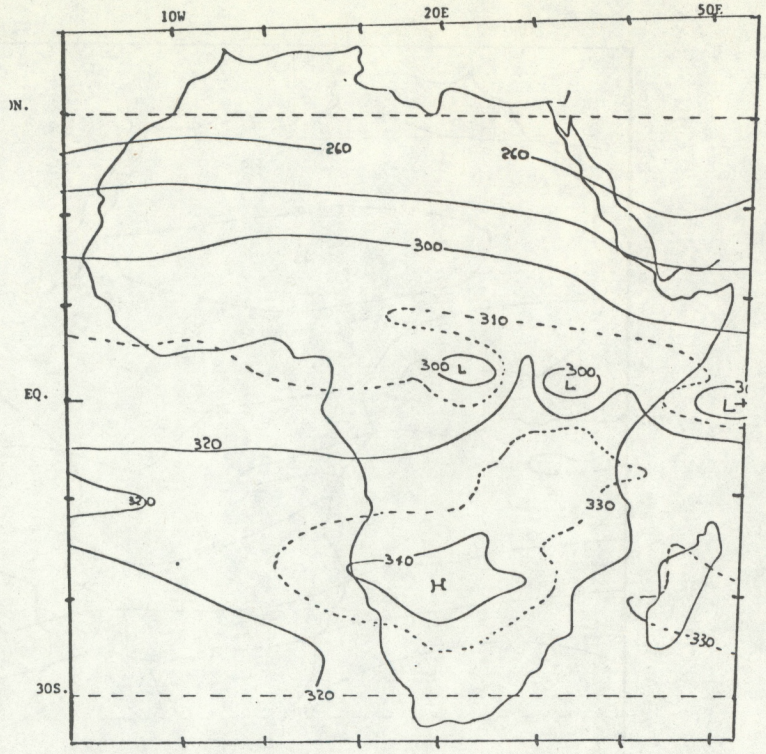

Figure 10d.--October.

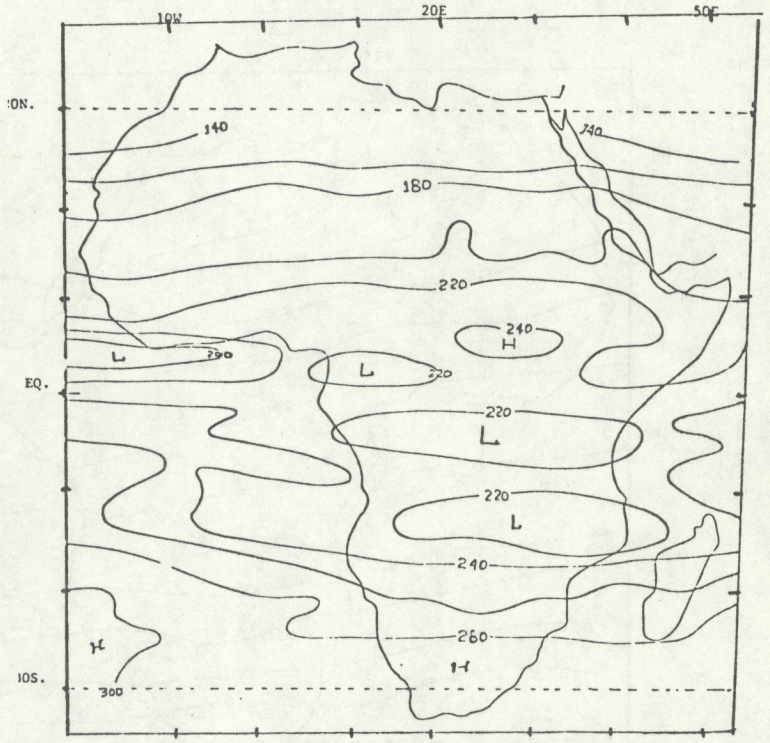

Figure 11.--Global solar radiation on a horizontal surface (W m^{-2}) estimated by ST-C method: (a) January.

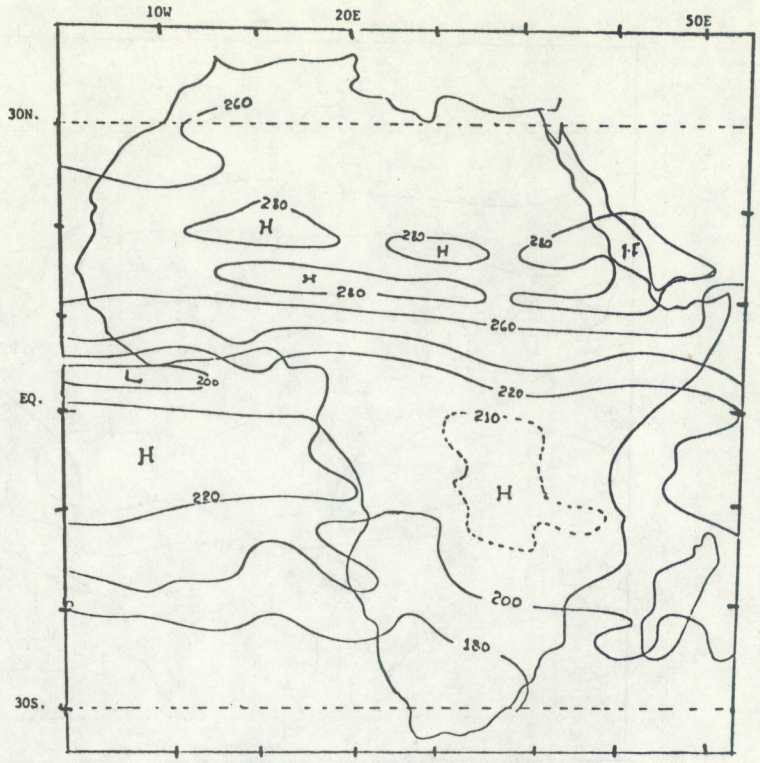

Figure 11b.--April.

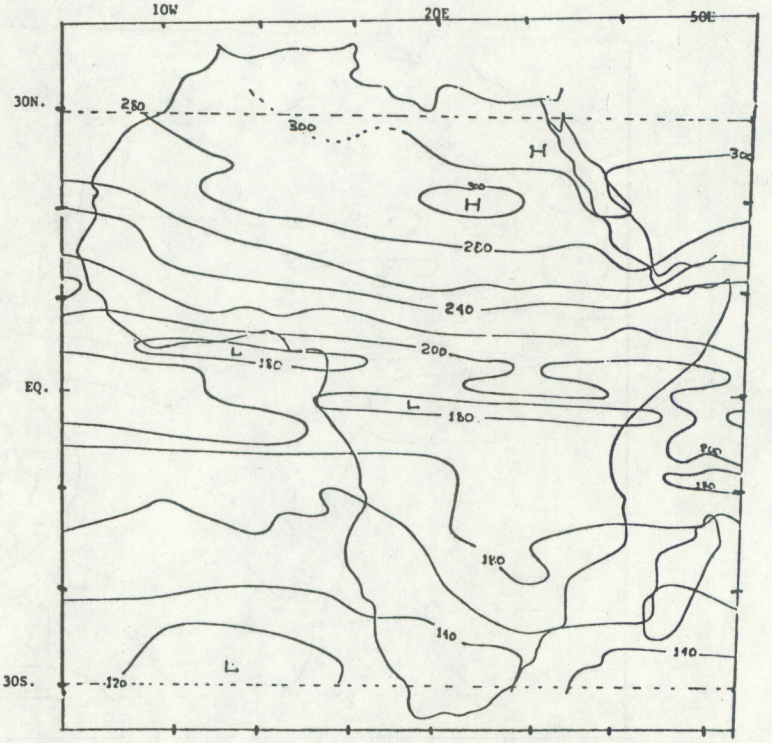

Figure 11c.--July.

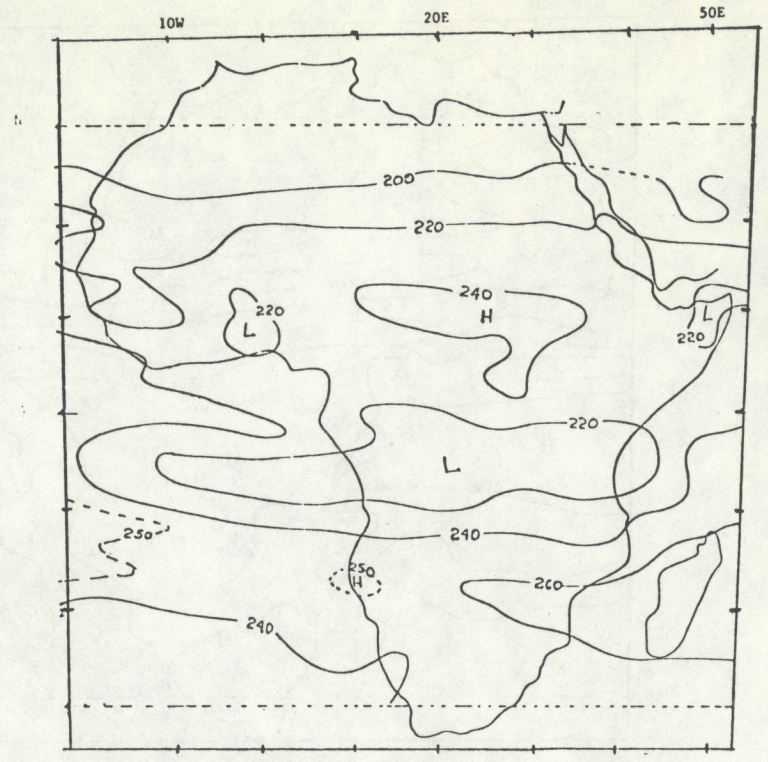

Figure 11d.--October.

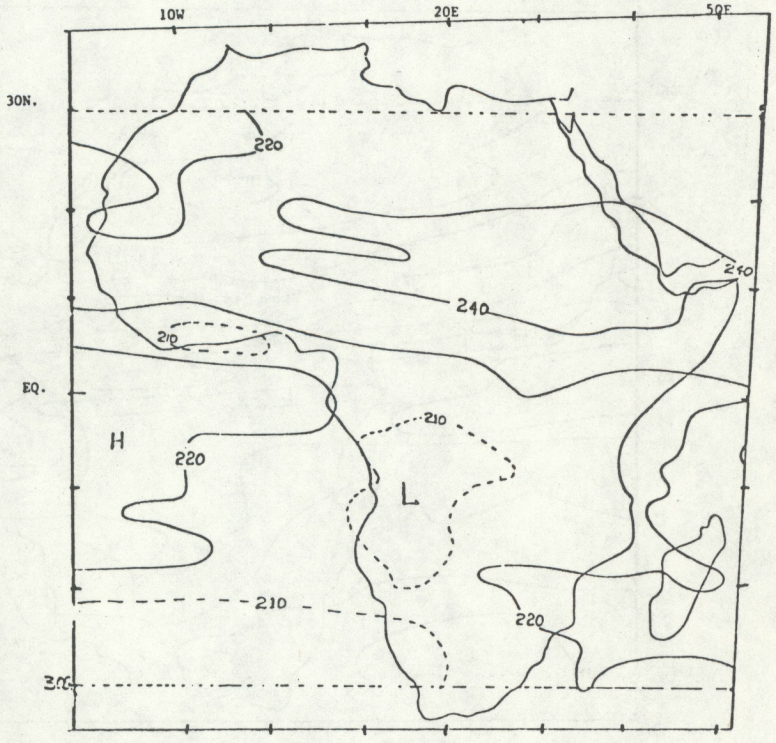

Figure 11e.--Annual.

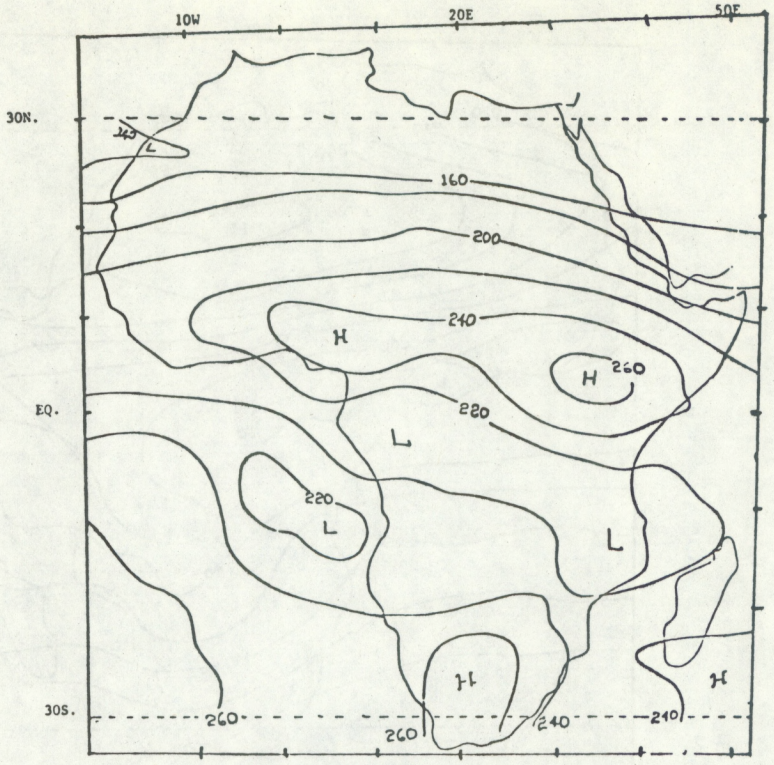

Figure 12.--Global solar radiation on a horizontal surface (W m^{-2}) estimated by the R method: (a) January.

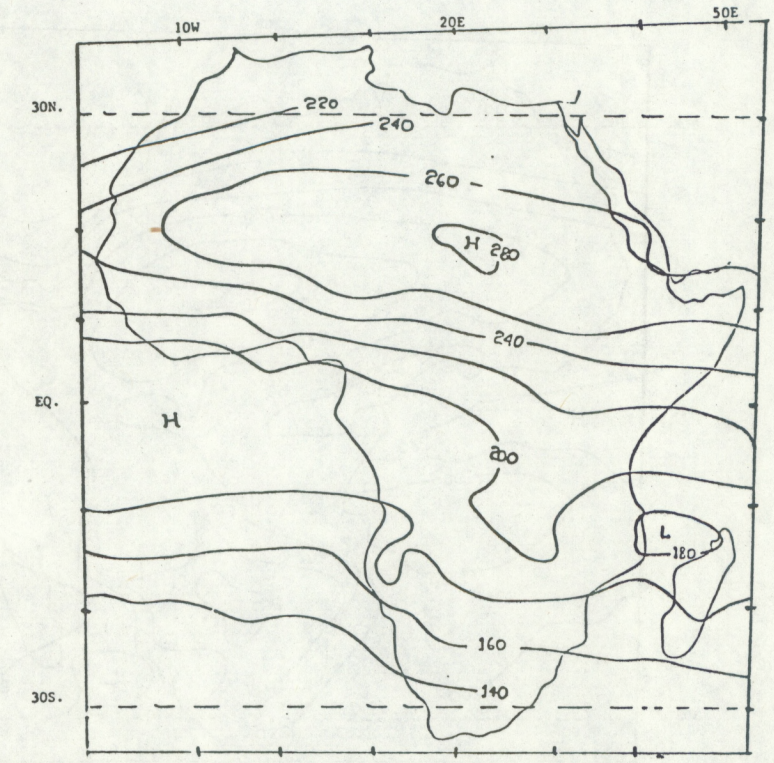

Figure 12b.--April.

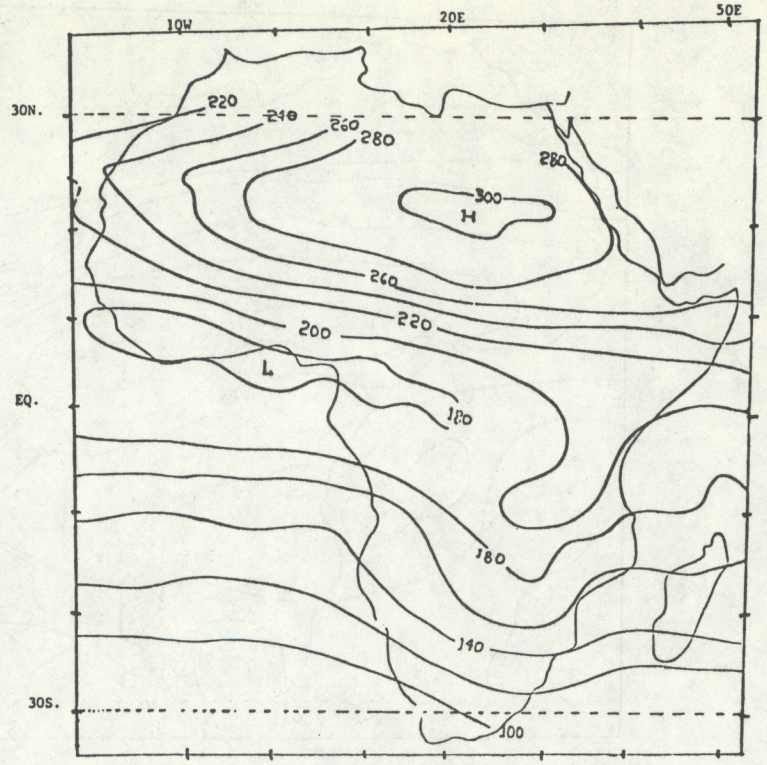

Figure 12c.--July.

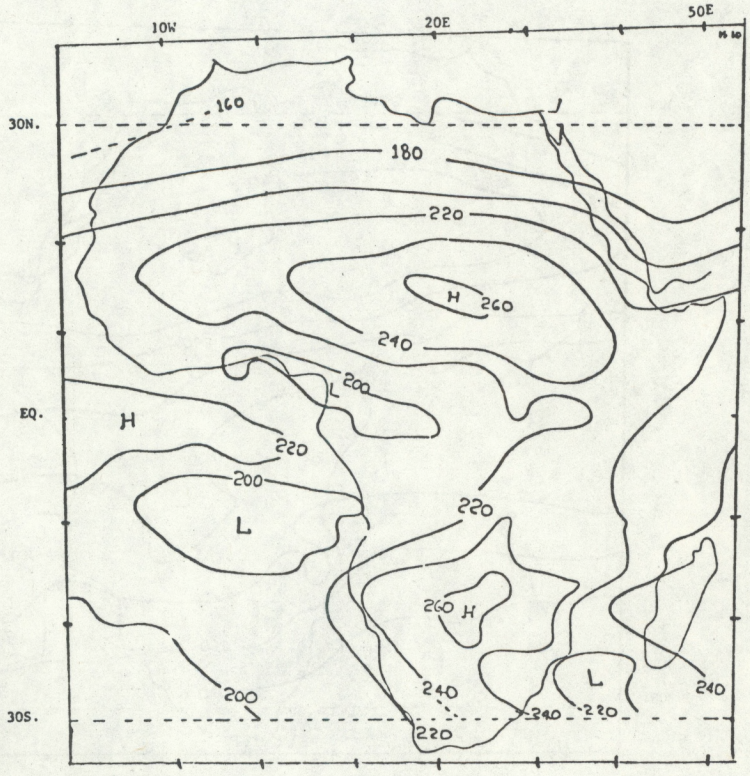

Figure 12d.--October.

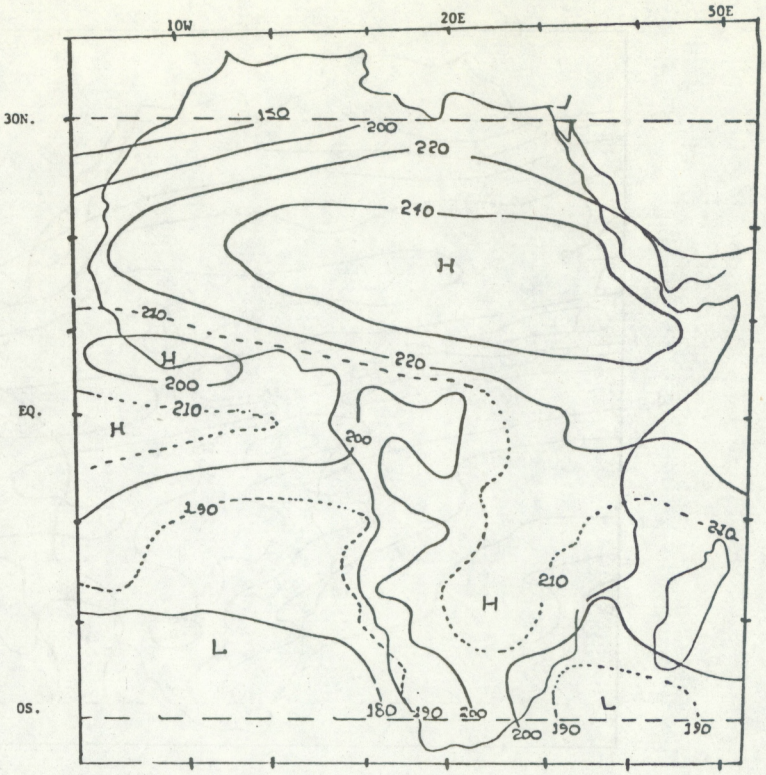

Figure 12e.--Annual.

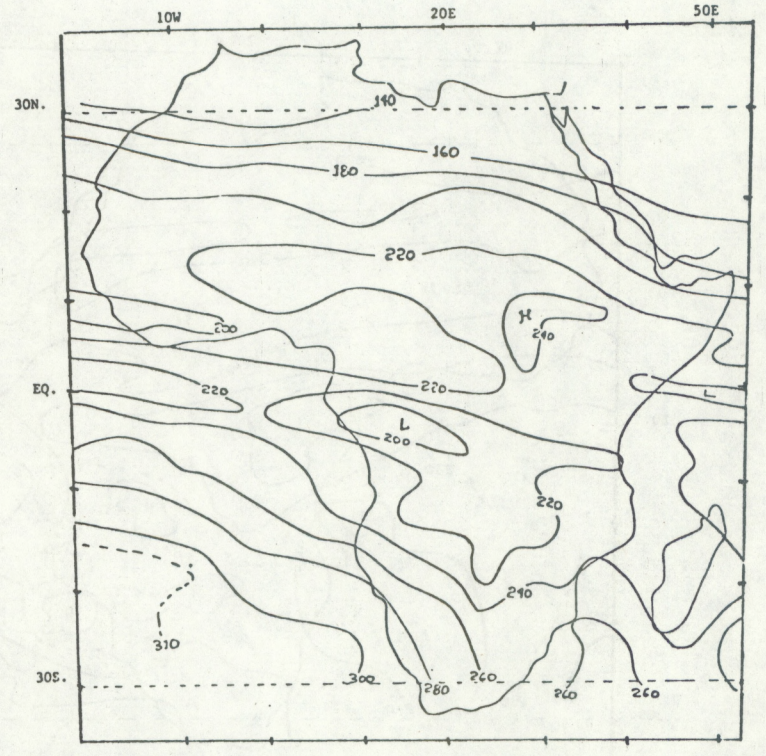

Figure 13.--Global solar radiation on a horizontal surface (W m^{-2}) estimated by the ST-CS method: (a) January.

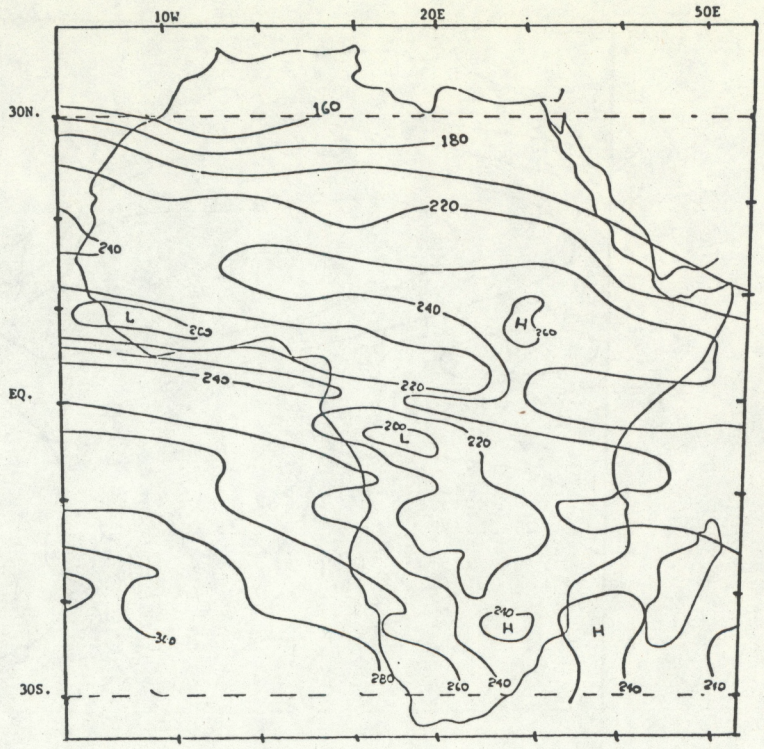

Figure 13b.--February.

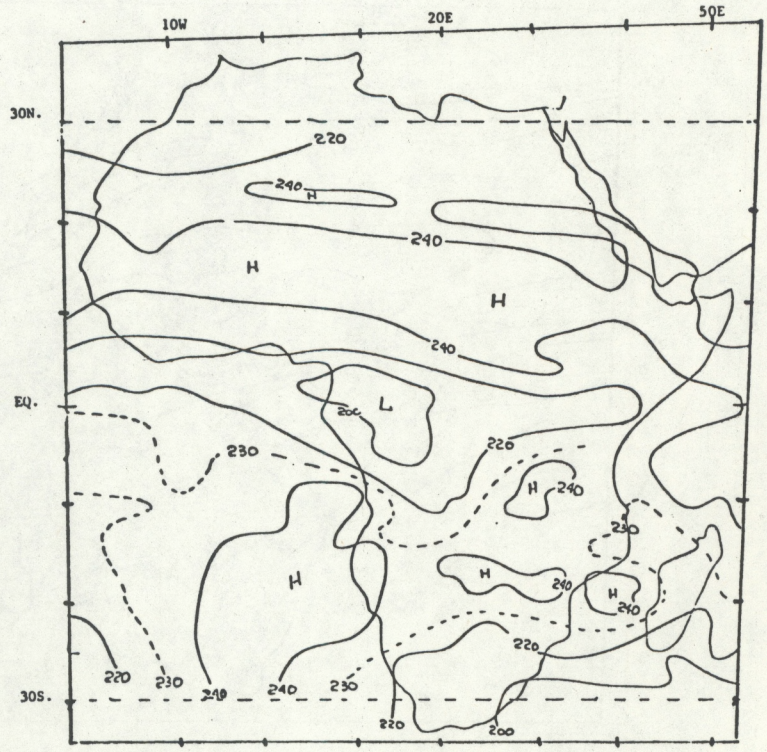

Figure 13c.--March.

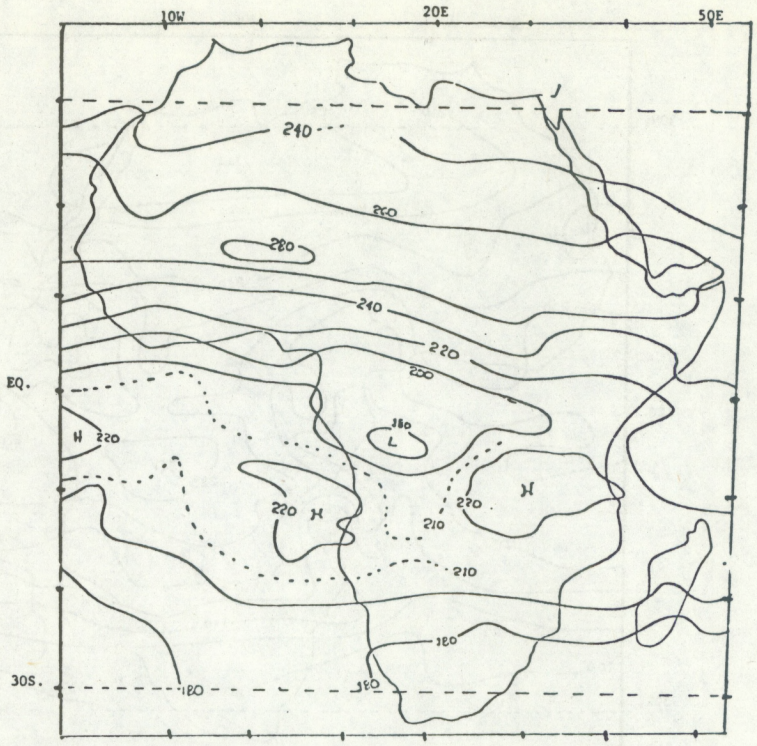

Figure 13d.--April.

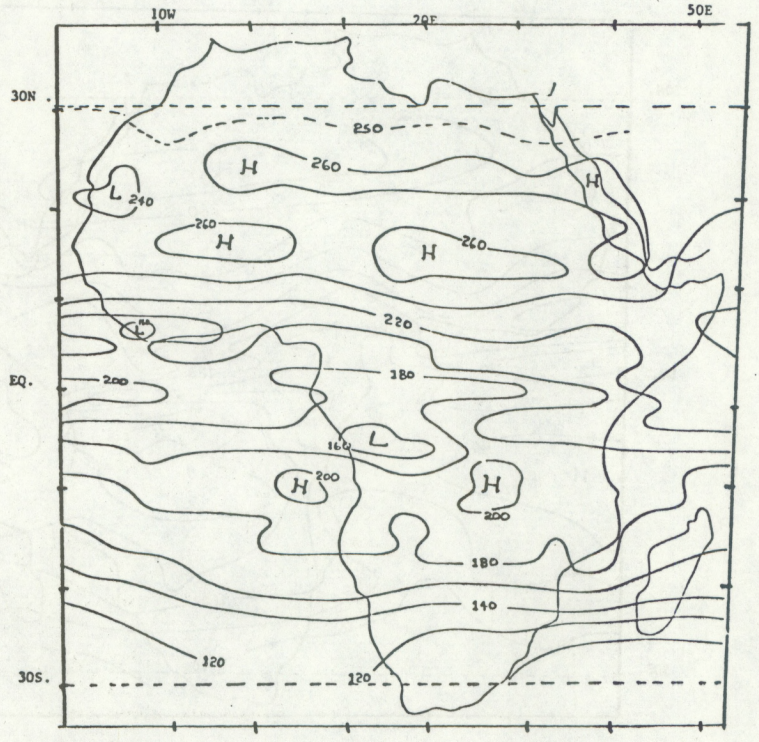

Figure 13e.--May.

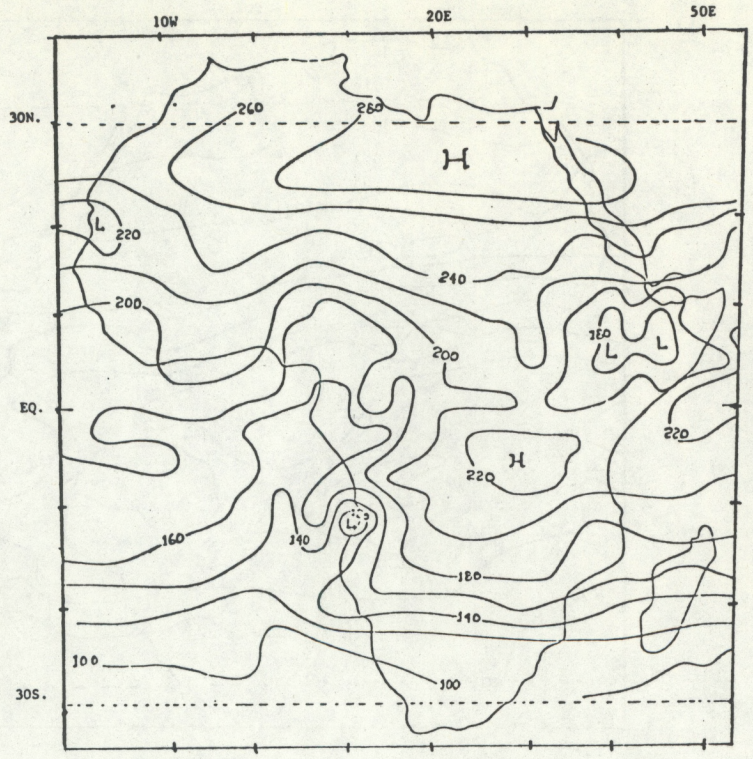

Figure 13f.--June.

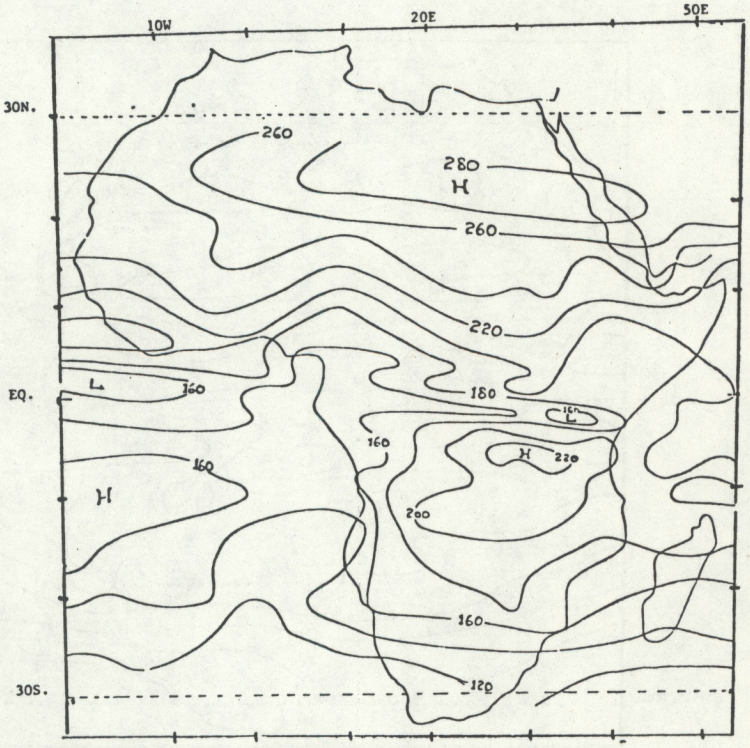

Figure 13g.--July.

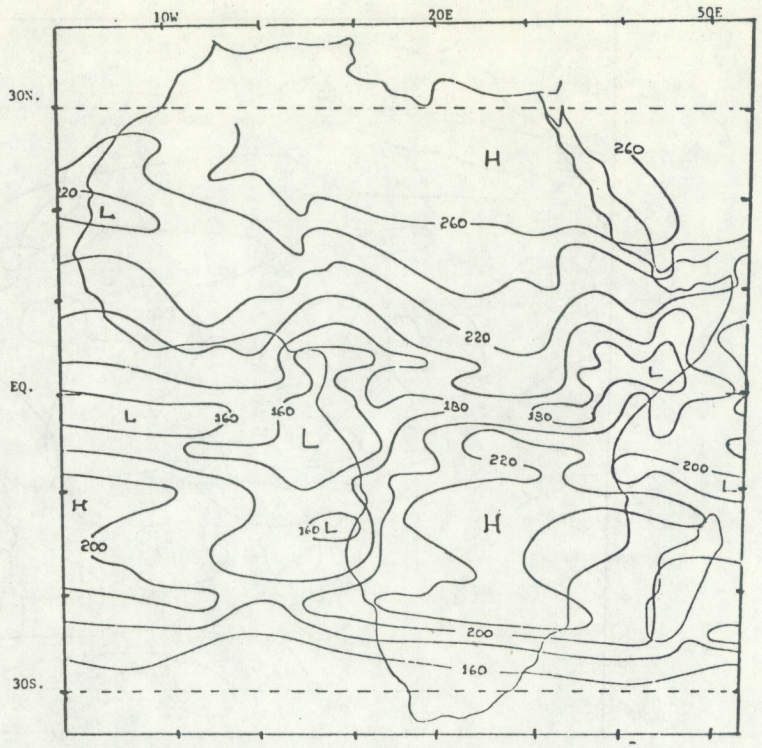

Figure 13h.--August.

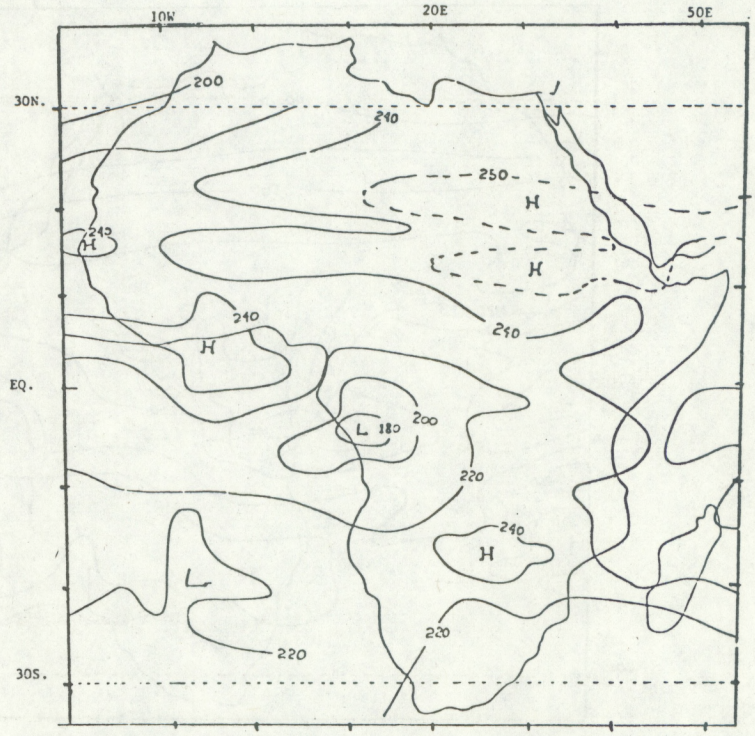

Figure 13i.--September.

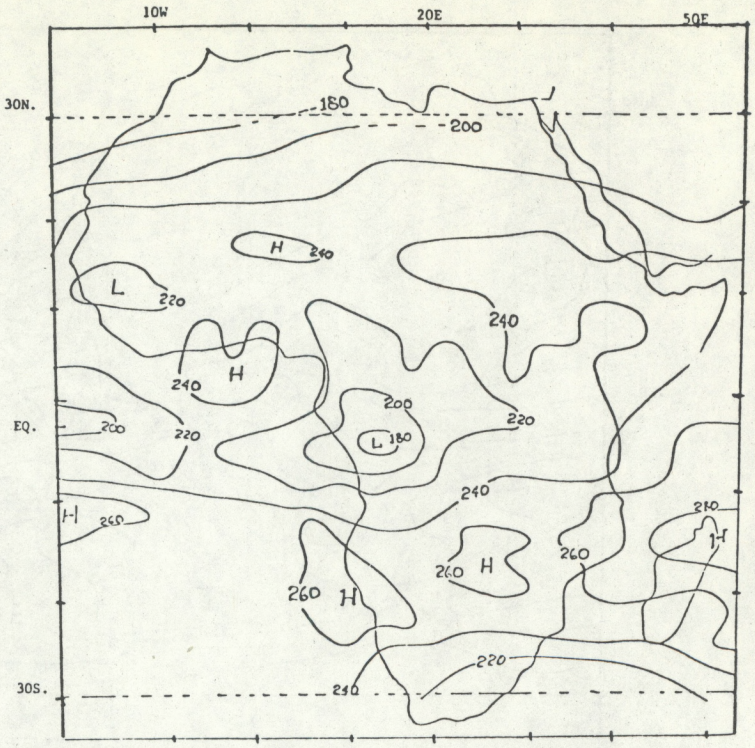

Figure 13j.--October.

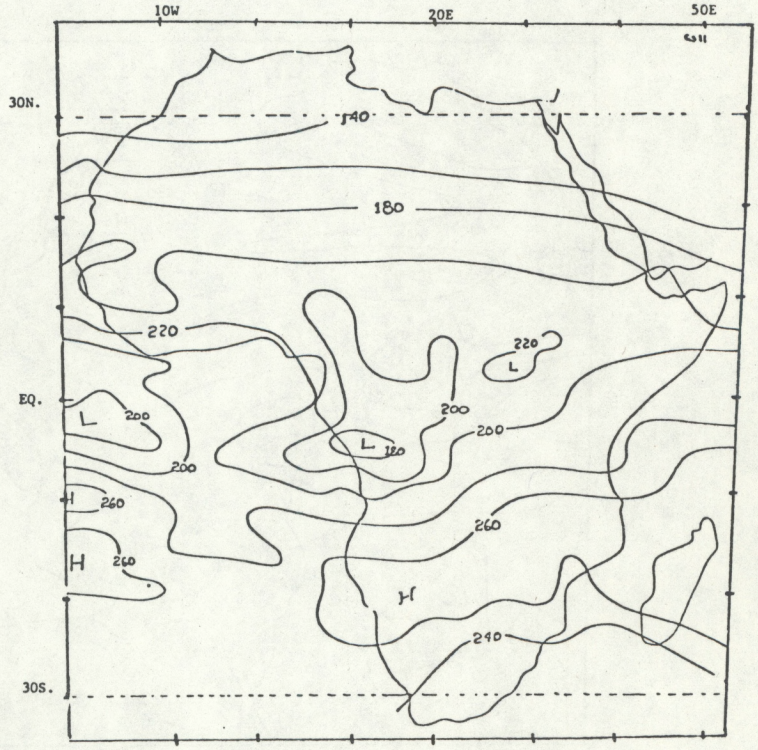

Figure 13k.--November.

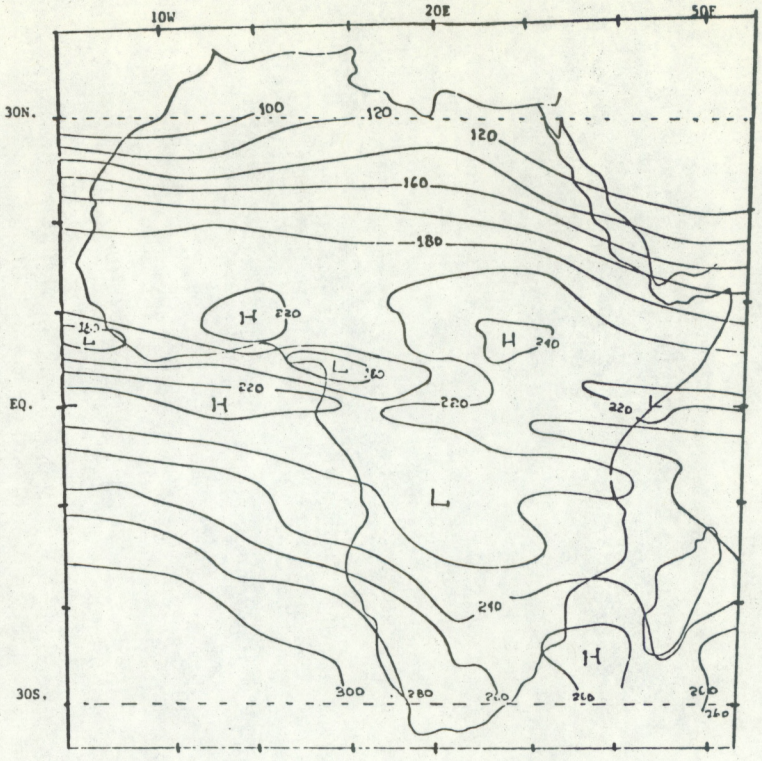

Figure 131.--December.

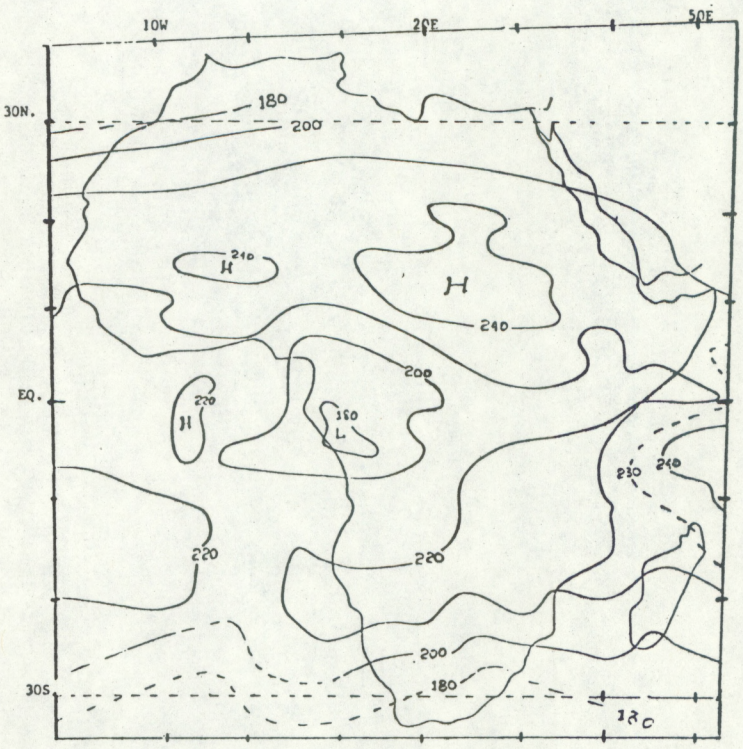

Figure 13m.--Annual.